creative commons

COMMONS DEED

저작자표시-비영리-변경금지 2.0 대한민국

이용자는 아래의 조건을 따르는 경우에 한하여 자유롭게

- 이 저작물을 복제, 배포, 전송, 전시, 공연 및 방송할 수 있습니다.

다음과 같은 조건을 따라야 합니다:

저작자표시. 귀하는 원저작자를 표시하여야 합니다.

비영리. 귀하는 이 저작물을 영리 목적으로 이용할 수 없습니다.

변경금지. 귀하는 이 저작물을 개작, 변형 또는 가공할 수 없습니다.

- 귀하는, 이 저작물의 재이용이나 배포의 경우, 이 저작물에 적용된 이용허락조건을 명확하게 나타내어야 합니다.
- 저작권자로부터 별도의 허가를 받으면 이러한 조건들은 적용되지 않습니다.

저작권법에 따른 이용자의 권리는 위의 내용에 의하여 영향을 받지 않습니다.

이것은 이용허락규약(Legal Code)을 이해하기 쉽게 요약한 것입니다.

Disclaimer

dCollection

Master's Thesis of Science in Agriculture

CRISPR Based Disease Mouse Model; Study for Genome Editing Efficiency of Campylobacter Jejuni Cas9 and In Vivo Gene Targeting for Pancreatic Cancer

CRISPR 기반의 질환 모델 마우스; 캠필로박터 제주니의 유전자 교정 효율 분석 및 생체 내 유전자 적중을 통한 췌장암 모델 확립연구

February 2018

Yoo Jin Chang

Department of International Agricultural Technology

Graduate School of International Agricultural Technology

Seoul National University

Abstract

CRISPR/Cas system has been a powerful tool for genome engineering which led to tremendous development in biological study. CRISPR/Cas Type II *inter alia, Streptococcus pyogene Cas9 (SpCas9)* was the first and widely used orthologue because it shows high cleavage efficiency of double strand DNA (dsDNA) and low off-target effect. Recently, novel orthologue *campylobacter jejuni* Cas9 (CjCas9) was reported as the smallest Cas9. Discovering novel orthologue is drawing attention because this doesn't just stop on finding new type of CRISPR it gives prospects for various application such as disease animal modeling and gene therapy. In addition, ultimate goal for overall applications is to cure genetic disease in human. Therefore, as the research advances high cleavage efficiency as well as low off-targets are being emphasized for CRISPR system. So in this study I focused on testing overall efficacy of SpCas9 and CjCas9 through animal modeling.

Firstly, by using classical orthologue SpCas9, I targeted *Hr* gene to generate hairless mouse. With using 4 sgRNAs in exon 3, cleavage activity revealed 30% (3/10) in blastocyst and 20-28.5% (1/5-2/7) in pup. Among the mutant pups, #1-4 mice (-3 and -34 amino acid deletion) and #2-4 mice (premature termination codon(PTC) and -50 amino acid deletion in genomic locus) were germline transmitted to observe phenotype. In #2-4 mice line, hairless phenotype was appeared about 2week postpartum whereas #1-4 mice line didn't showed the hair loss. This study verified SpCas9 cleavage activity and in addition it suggests appropriate model for dermatological research and *in vivo* imaging.

During our study novel orthologue CjCas9, briefly stated above, was reported. However previous studies were conducted in in vitro and overall efficacy were not established. Albeit several opinions of cleavage ability about CjCas9, I investigated cleavage efficiency as well as off-target possibilities in *in vivo*. Totally, in zygote and

generated mice cleavage efficiency showed 38-100% which showed unexpected high rate. Besides off-target analysis showed ≤1.6% which indicates high specificity. In addition, most recent report related to off-target analysis using bioinformatics study conducted by Schaefer *et al* demonstrated high off-targets in SpCas9. However, on the line of our study with CjCas9 I found this was a misleading interpretation due to aligning SpCas9 mediated mutant mice sequence to wrong control mice sequence. Consequently, CjCas9 showed high cleavage efficiency as well as high specificity and this suggests safe gene targeting which can broaden biological development.

With our discovery of efficiency and accuracy in CjCas9, I applied it to multiple gene related pancreatic cancer modeling with *in vivo* gene targeting mediated by adeno-associated virus (AAV). In this study, 5 genes (*Kras, Ink4a, Tp53, Smad4, Brca2*) related to pancreatic cancer were selected and SpCas9 and CjCas9 were directly compared by targeting same genes. Cleavage rate were confirmed in zygote and it revealed similar rate between SpCas9 and CjCas9. Then, *in vivo* gene targeting in adult mice was proceeded by directly injecting AAV packaged molecule into pancreas common bile duct. After surgery monitoring were conducted every week and since cancer formation takes at least 9month post-surgery, this studies are ongoing.

In conclusion, I demonstrate safe and stable ability in CjCas9 as well as SpCas9 by generating animal model in various way. This suggest prospects for broad application.

Key words: Animal model, *Campylobacter jejuni*, CRISPR, Hairless, in vivo gene targeting, Pancreatic cancer

Student number: 2016-20018

Contents

Abstract…….. i

Contents……..iii

List of Tables…….....vi

List of Figures……vii

List of Abbreviation…….....ix

Chapter I: Generation of Hairless mouse using CRISPR/Cas9 system

1. Introduction……..1
2. Material and method……3
   - 2.1. Animal
   - 2.2. Preparation of Cas9 mRNA and sgRNA
   - 2.3. Microinjection into embryos
   - 2.4. Genotyping and sequencing
   - 2.5. Germline transmission
3. Results……..9
   - 3.1. sgRNA efficiency test in C57BL/6 embryos
   - 3.2. Generation of hairless mouse by CRISPR/Cas9

3.3. Germline transmission

3.4. Hairless Phenotype

4. Discussion……..19

Chapter 2 : Whole Genome Sequencing of Genome Modified mice generated with *Campylobacter jejuni* Cas9 reveals High Specificity of CRISPR/Cas9

1. Introduction……....……23

2. Material and method……..……26

2.1. Animal

2.2. Preparation of Cas9 mRNA and sgRNA

2.3. Embryo microinjection

2.4. Genotyping and sequencing

2.5. In silico design of Off-target sites

2.6. Targeted deep sequencing

2.7. Whole genome sequencing

3. Results……..…….....34

3.1. High cleavage activity of CjCas9 in knock out mice generation

3.2. Off-target Analysis showed high specificity

3.3. WGS based bioinformatics analysis revealed different off-target rate by the control mice

4. Discussion……..…...…….47

Chapter 3 : In vivo Multiple Gene Targeting with *Campylobacter jejuni* cas9 for Pancreatic Cancer

1. Introduction……51

2. Material and method……..……53

2.1. Target gene sgRNAs preparation

2.2. Generation of SpCas9 overexpression mice

2.3. Vector Preparation of AAV2-SpCas9 and AAV2-3sgRNAs

2.4. AAV preparation

2.5. AAV injection into pancreas

3. Results……..…….....61

3.1. SgRNA cleavage activity test of SpCas9 and CjCas9 in C57BL/6 embryo

3.2. SpCas9 expression was confirmed by RFP signal in pancreas

3.3. In vivo Pancreas-tropism of AAV2

3.4. Monitoring

4. Discussion…….…….73

References……..……77

국문초록……..……..83

감사의 글…….85

List of Tables

Table 1. sgRNA target region……..……5

Table 2. PCR Primer sets for genotyping.…….……..7

Table 3. Summary of Hairless KO mice generation……...…..12

Table 4. sgRNA sequences used in this study……...……..28

Table 5. Primer sequences for genotyping used in this study……..….30

Table 6. List of primers used for targeted deep sequencing……...……..32

Table 7. Summary of CjCas9 mediated KO and KI mice generation…….....35

Table 8. Off target sites for CjCas9 targeted *Try* and *Foxn1* genes……42

Table 9. sgRNA target region.……...……..54

Table 10. Summary of in vivo gene targeting group…….……60

Table 11. PCR Primer sets for genotyping.……...……66

List of Figures

Figure 1. Structure of p3s-Cas9 ……..……..4

Figure 2. Evaluation of sgRNA efficacy……..10

Figure 3. *Hr* KO mice generation with SpCas9.……13

Figure 4. Analysis of gene expression in line Founder #2-4……..……..17

Figure 5. Structure of pCMV-CjCas9-pA. …….……27

Figure 6. *Tyr* KO mice generation with CjCas9. ……...…….36

Figure 7. *Foxn1* KO mice generation with CjCas9. ……...……39

Figure 8. Bioinformatics study with WGS. ……...……45

Figure 9. pAAV-3sgRNA modification strategy. ……..……57

Figure 10. Schematic for pancreatic cancer modeling and Cas9 overexpression mouse…….……62

Figure 11. Evaluation of sgRNA efficacy. ……..…….65

Figure 12. Cas9 overexpression mouse validation by RFP signal……..68

Figure 13. pAAV-GFP in vivo gene targeting ex vivo imaging……..…….70

Figure 14. pAAV-GFP in vivo gene targeting ex vivo imaging…….……..71

List of Abbreviations

AAV	adeno associated virus
AmpR	Ampicillin Resistance
bp	base pair
C57BL/6	C57 Black 6 mice
Cap	Capsid
Cas9	CRISPR associated protain 9
CjCas9	*Campylobacter Jejuni* Cas9
CMV	Cytomegalovirus promoter
CPF1	Centromere and Promoter Factor 1
CRISPR	Clustered Regularly Interspaced Short Palindromic Repeats
crRNA	CRISPR RNA
DNA	Deoxyribonucleic acid
DSB	Double strand Break
EF-1	EF-1-alpha core promoter
F0	Founder
F1	First Filial generation
F1 ori	F1 bacteriophage origin of replication
F2	Second Filial generation
FGFR1	Fibroblast growth factor receptor 1
Foxn1	Forkhead box N1
FVB	Friend Virus B-Type mouse
G12D	12th Glycine changed to Aspartic acid
GFP	Green fluorescent protein

GOI	Gene of Interest
gRNA	guide RNA
HDR	Homologous Direct Repair
HEK293T	Human Embryonic Kidney 293T
Hr	Hairless
HSPG	Heparan Sulfate Proteoglycan
ICR	Institute for Cancer Research mice
Indel	Insertion Deletion
ITR	Inverted terminal repeat
KI	Knock-in
KO	Knockout
LSL	Loxp Stop Loxp
N	Number
NGS	Next Generation Sequencing
NHEJ	Non Homologous End Joining
ORI	Origin of Replication
pA	poly Adenylation
PAM	Protospacer Adjacent Motif
PB-pCAG-spCas9/RFP-polyA	Piggybac-CMV enhancer, chicken beta Actin promoter and rabbit beta Globin splice acceptor-*Streptococcus Pyogenes* Cas9/Red Fluorescent Protein-poly Adenylation
PCR	Polymerase Chain Reaction
PDAC	Pancreatic Ductal Adenocarcinoma
psgRNA	plasmid single guide RNA
PTC	Premature Termination Codon

qPCR	Quantitative Polymerase Chain Reaction
R172H	172nd Arginine changed to Histidine
Rep	Replication
RNA	Ribonucleic acid
SEM	Standard Error of the Mean
sgRNA	Single Guide RNA
SNP	Single Nucleotide Polymorphism
SNV	Single Nucleotide Variation
SpCas9	*Streptococcus Pyogenes* Cas9
T7E1	T7 Endonuclease 1
TALEN	Transcription Activator Like Effector Nuclease
TG	Transgenic
tracrRNA	Trans-activating crRNA
Tyr	Tyrosinase
WGS	Whole Genome Sequencing
ZFN	Zinc Finger Nuclease

Chapter I

Generation of Hairless mouse using CRISPR/Cas9 system

1. Introduction

Genome engineering has been gone through rapid improvement ever since site-directed zinc finger nucleases (ZFNs) and TAL effector nucleases (TALENs) using the principles of DNA-protein recognition were developed. Recently, clustered regularly interspaced short palindromic repeat (CRISPR)/ CRISPR associated protein enabled simple, less time-consuming and high efficient gene targeting[1]. Briefly, CRISPR/Cas system is an RNA mediated adaptive immune defense system which exist in archaea and bacteria to degrades foreign genetic materials such as viruses and plasmids[2-7]. In prokaryote organism who uses this system integrates sequence information that previously encountered invading nucleic acid in CRISPR locus[8, 9]. This system is utilized for manipulating eukaryotic cells by recognizing specific sequence site and guides to direct cleavage of complementary DNA via the nuclease activity of CRISPR-Cas9 protein[10, 11].

In many orthologues in CRISPR/Cas9 type II CRISPR *Streptococcus pyogenes* Cas9 (SpCas9) is widely used. SpCas9 has simple proto-spacer adjacent motif (PAM)[12] which is 5'-NGG-3' and shows high cleavage efficiency. Even preparing molecule is simple so it became convenient tool for generating either knockout or knock-in mouse model.

Hairless (*Hr*) gene is widely used target because of its accurate and easily detectable phenotype. Also, in many research fluorescence or luminescence molecules are commonly used in *in vivo* imaging for diagnostics. However, the hair

makes lights scatter, block, and absorb. Besides, black hair absorbs more light than other color hairs [13, 14]. So, it is necessary to remove the hair to detect signals with *in vivo* imaging system. So far, *Hr* knockout mouse was generated by spontaneous or chemically induced. Although there was a few knockout mouse generated by targeting, it was based on ES cells (Embryonic stem cells).

To generate optimal animal model for in vivo imaging I decide to knockout *Hr* gene and induce hair loss in mice. Here I produce hairless mice with *streptococcus pyogenes* CRISPR/Cas9 without time-consuming endeavor. We used 4 sgRNAs to induce double strand break (DSB) and CRISPR/Cas9 molecules are injected into C57BL/6 embryos. To acquire homozygous, germline transmission was conducted. As a result, I observed clear phenotype in frameshifted mice whereas indel mice without frameshift didn't show hair loss.

1. Materials and Method

2.1 Animal

C57BL/6 mice were obtained from Koatech (Pyeongtaek, Korea). All mice were maintained in individual ventilated cages and given access to food and water *ad libitum*. This study was approved by the Institutional Animal Care and Use Committees of Seoul National University (SNU-171115-9) and was conducted in accordance with approved guidelines.

2.2 Preparation of Cas9 mRNA and sgRNA

The p3s-Cas9HC plasmid was obtained from Addgene (Cambridge, MA, USA). Briefly, p3s-Cas9 was linearized by XbaI enzyme cutting and DNA was collected by purification kit (Qiagen, Hilden, Germany). In vitro capped transcription and polyadenylation tailing were conducted with mMESSAGE mMACHINE T7 ultra kit (Thermo Fisher Scientific, Waltham, MA, USA) according to instruction. Brief structure of p3s-Cas9HC is shown in Figure 1. sgRNAs were designed by chopchop[15] according to its PAM sequence(5'-NGG-3'). Then sgRNAs were synthesized using an in vitro RNA synthesis kit (Thermo Fisher Scientific, Waltham, MA, USA) following PCR amplification. Detail sgRNA sequences are listed in Table1.

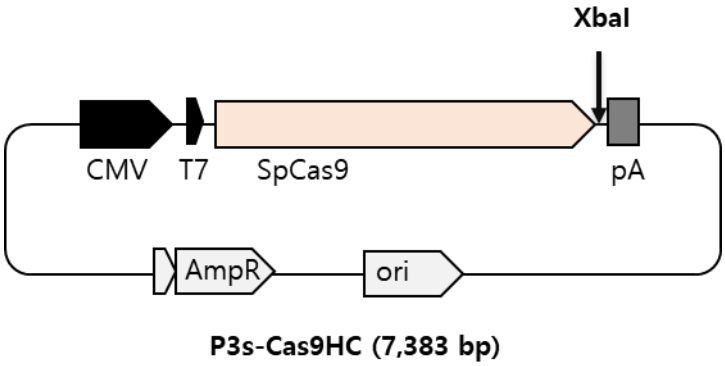

Figure 1. Structure of p3s-Cas9. Plasmid includes CMV enhancer and promoter (584 bp), T7 promoter (19 bp), SpCas9 (4104 bp) and bovine growth hormone polyadenylation signal sequence (225 bp). XbaI enzyme site exist as unique cutter which used for linearization.

Table 1. sgRNA target region.

sgRNA	Target sequence	Genomic location	Exon	GC content (%)	Off-targets		
					0	1	2
1	AGAGTGACCCTGTGGCCTTCCGG	chr14:70556783	3	65	0	0	0
2	GGAAAGGGCAGTGCAAGGGCCGG	chr14:70556802	3	70	0	0	0
3	GCCAGTCATATGGACGCTCTGGG	chr14:70556904	3	61	0	0	0
4	GGCCTTTGGCCCCAAACCCATGG	chr14:70556924	3	65	0	0	0

2.3 Microinjection into embryos

C57BL/6 female mice were superovulated by injecting pregnant mare's serum gonadotropin (Prospec Bio, East Brunswick, NJ, USA) and human chorionic gonadotropin (Prospec) for 46~48hour interval, and embryos were collected in M2 medium (MTI-Global stem, Rockville, MD, USA) at next day. Then, embryos were incubated in KSOM medium (Merk Millipore, Billerica, MA, USA) for 3 hour and normal fertilized embryos with 2 pronucleus were selected and microinjection was conducted with micromanipulator (Eppendorf, Hamburg, Germany). Briefly, 50ng/μL of Cas9 mRNA, 10 ng/μL for each sgRNAs were mixed, and microinjected into embryos. After embryos were cultured to 2-cell stage and transferred into pseudo-pregnant female or cultured until blastocyst stage for genotyping.

2.4 Genotyping and sequencing

DNA was extracted from blastocyst, and toe clip of pups. Single embryos were transferred to 250μL PCR tubes filled with 20μL distilled water by mouth pipette, and used as templates for PCR after 3 times freeze-thaw and denaturation in at 95ºC for 15 min. DNA extraction from toe sample was conducted with using gRNA extraction kit (Intron Bio, Kyungki-Do, Korea). After PCR reaction, amplicons were used for T7E1 analysis (NEB, Ipswich, MA, USA) or used for TA cloning and Sanger sequencing (Cosmo Genetech, Seoul, Korea). Primers for genotyping are listed in Table 2.

Table 2. PCR Primer sets for genotyping.

Target gene	Primer	Product size (bp)	Annealing Tm (ºC)
Hr	F: 5’- CTTTTGGAGGGGTGTTCTG -3’ R: 5’- CCCACTGTATTTCGTCACT -3’	491	56

2.5 Germline transmission

The Founder mouse(F_0) which has premature termination codon(PTC) was selected for germline transmission. Since F_0 was heterozygous, mating was proceeded with wild type mouse. After genotyping offspring (F_1) from F_0, heterozygous mice were selected and mated each other once more to acquire homozygous mice (F_2). I monitored every day for hair loss phenotype in homozygous mice.

2. Results

3.1 sgRNA efficiency test in C57BL/6 embryos

To induce large sized DSB in the Hairless (*Hr*) gene, 4 sgRNAs with 20 nucleotide(nt) sized and 5'-NGG-3' PAM in exon 3 was selected. 4sgRNAs were paired into 2 part and distance between each pair was 74bp (Fig.1a). Next, I microinjected SpCas9 mRNA and sgRNAs into C57BL/6 embryos, and conducted PCR based genotyping. Of total 10 embryos, 10 embryos were successfully genotyped, and they showed 30% (3/10) of cleavage rate (Figure 2).

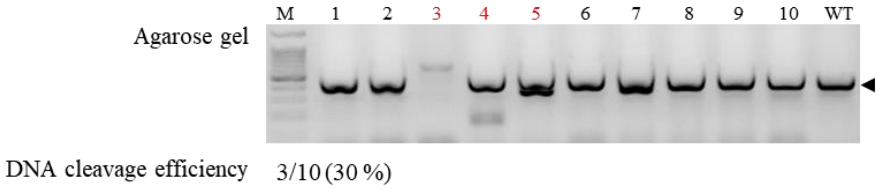

Figure 2. **Evaluation of sgRNA efficacy.** sgRNAs and cas9 mRNA were co-injected into 1-cell embryos and DNA cleavage activity were evaluated in blastocyst. Blastocyst genotyping showed 3/10 (30%) of DNA cleavage efficiency. Black arrow indicates wild type target size (491 bp). Detail information about primer is in Table 2.

3.2 Generation of hairless mouse by CRISPR/Cas9

After confirming targeting efficiency, 2 times of microinjection-embryo transfer was conducted. At 1st trial (Pups-#1), 55 microinjected embryos were transferred into surrogate dam and 5 pups were obtained and at 2nd trial (Pups-#2), 136 microinjected embryos were transferred into surrogate dam and 7 pups were obtained (Table 3). PCR and T7 endonuclease (T7E1) based genotyping with pups-#1 and pups-#2 result exhibited 20%(1/5) and 28.5% (2/7) of cleavage efficiency respectively (Figure 3b and Table 3) which was lower than in blastocysts level.

Table 3. Summary of Hairless KO mice generation

Gene	Type	No of injected embryo	No. of 2 cell stage embryo (%)	No. of BL (%)	No. of transferred embryos	No. of offsprings (%)	Targeting efficiency (%) (No. of mutant/total blastocysts or offsprings)
Hr	Embryo test	25	17 (68)	10 (58.8)	NA	NA	30 (3/10)
	1st pup	70	56 (80)	NA	55	5 (9)	20 (1/5)
	2nd pup	254	212 (83)	NA	136	7 (5.1)	28.5 (2/7)

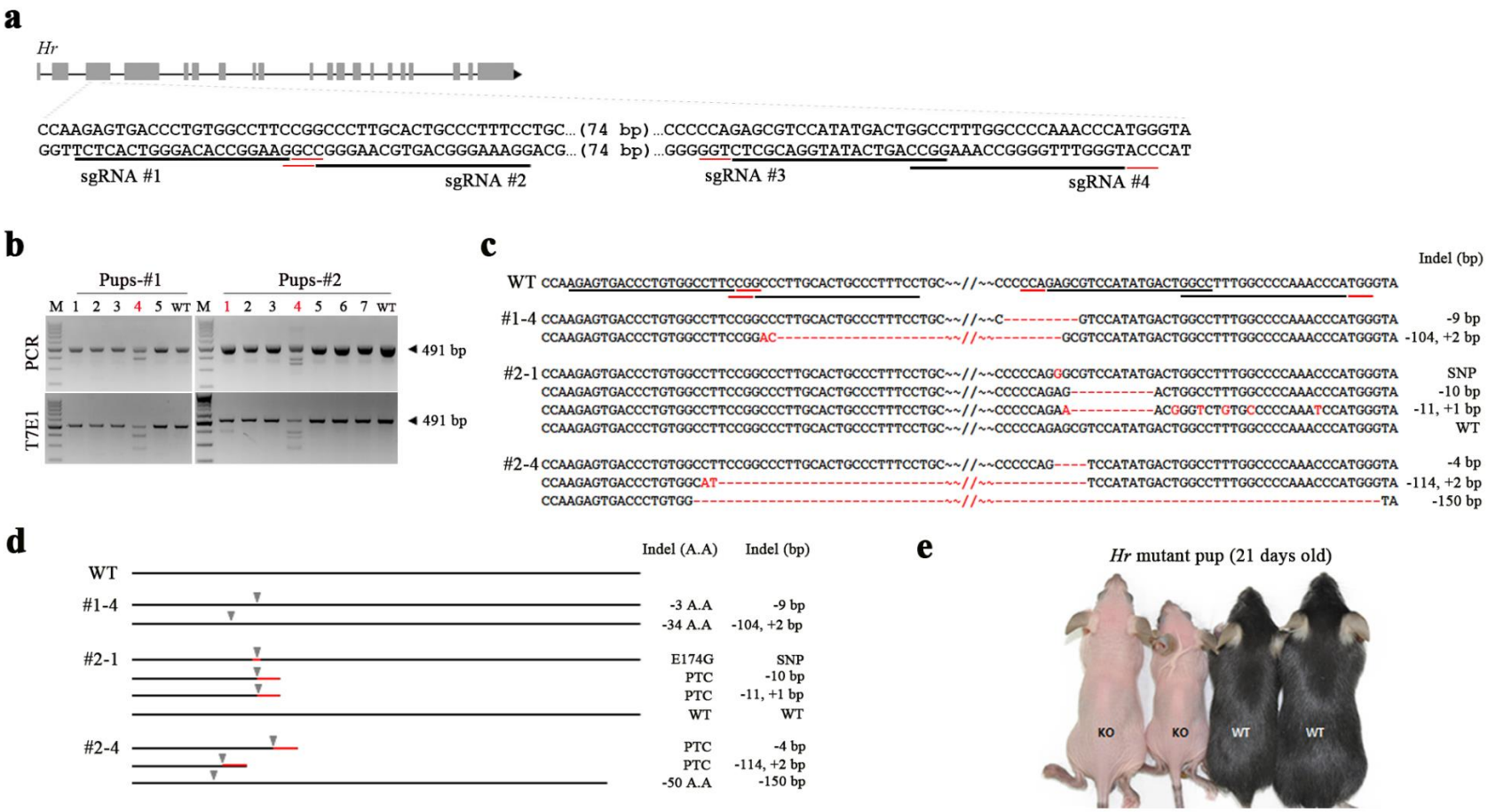
a
Hr
CCAAGAGTGACCCTGTGGCCTTCCGGCCCTTGCACTGCCCTTTCCTGC...(74 bp)...CCCCCAGAGCGTCCATATGACTGGCCTTTGGCCCCAAACCCATGGGTA
GGTTCTCACTGGGACACCGGAAGGCCGGGAACGTGACGGGAAAGGACG...(74 bp)...GGGGGTCTCGCAGGTATACTGACCGGAAACCGGGGTTTGGGTACCCAT
sgRNA #1
sgRNA #2
sgRNA #3
sgRNA #4
b
Pups-#1
Pups-#2
M 1 2 3 4 5 WT M 1 2 3 4 5 6 7 WT
PCR
T7E1
491 bp
491 bp
c
Indel (bp)
WT CCAAGAGTGACCCTGTGGCCTTCCGGCCCTTGCACTGCCCTTTCCTGC~~//~~CCCCCAGAGCGTCCATATGACTGGCCTTTGGCCCCAAACCCATGGGTA
#1-4 CCAAGAGTGACCCTGTGGCCTTCCGGCCCTTGCACTGCCCTTTCCTGC~~//~~C---------GTCCATATGACTGGCCTTTGGCCCCAAACCCATGGGTA -9 bp
CCAAGAGTGACCCTGTGGCCTTCCGGAC----------~~//~~---------GCGTCCATATGACTGGCCTTTGGCCCCAAACCCATGGGTA -104, +2 bp
#2-1 CCAAGAGTGACCCTGTGGCCTTCCGGCCCTTGCACTGCCCTTTCCTGC~~//~~CCCCCAGGGCGTCCATATGACTGGCCTTTGGCCCCAAACCCATGGGTA SNP
CCAAGAGTGACCCTGTGGCCTTCCGGCCCTTGCACTGCCCTTTCCTGC~~//~~CCCCCAGAG----------ACTGGCCTTTGGCCCCAAACCCATGGGTA -10 bp
CCAAGAGTGACCCTGTGGCCTTCCGGCCCTTGCACTGCCCTTTCCTGC~~//~~CCCCCAGAA----------ACGGGTCTGTGCCCCCAAATCCATGGGTA -11, +1 bp
CCAAGAGTGACCCTGTGGCCTTCCGGCCCTTGCACTGCCCTTTCCTGC~~//~~CCCCCAGAGCGTCCATATGACTGGCCTTTGGCCCCAAACCCATGGGTA WT
#2-4 CCAAGAGTGACCCTGTGGCCTTCCGGCCCTTGCACTGCCCTTTCCTGC~~//~~CCCCCAG----TCCATATGACTGGCCTTTGGCCCCAAACCCATGGGTA -4 bp
CCAAGAGTGACCCTGTGGCAT----------~~//~~----------TCCATATGACTGGCCTTTGGCCCCAAACCCATGGGTA -114, +2 bp
CCAAGAGTGACCCTGTGG----------~~//~~----------TA -150 bp
d
Indel (A.A)
Indel (bp)
WT
#1-4
-3 A.A -9 bp
-34 A.A -104, +2 bp
#2-1
E174G SNP
PTC -10 bp
PTC -11, +1 bp
WT WT
#2-4
PTC -4 bp
PTC -114, +2 bp
-50 A.A -150 bp
e
Hr mutant pup (21 days old)
KO
KO
WT
WT

Figure 3. *Hr* KO mice generation with SpCas9. (a) Schematic represent target site for gene targeting. Four sgRNAs with 20 nucleotide sequence of binding site (black line) were used, and red line indicate PAM sequence (5'-NGG-3'). Gray box indicate exon. (**b**) Pup was generated twice (#1, #2) and PCR and T7 endonuclease (T7E1) based analysis was conducted. Totally, 25% (3/12) mutant pup were obtained. Red letters indicate DNA cleaved pup. M: size marker, WT: wild type control. (**c**) Results of sequencing (#1-4, #2-1 and #2-4 founder) in each sgRNA binding sites. All mutant pup showed indels in sequencing result. Red "-" and red letters indicate deleted and inserted nucleotides, respectively. (**d**) Result of translation in the *Hr* gene. #1-4 showed simple amino acid deletion whereas #2-1 and #2-4 showed premature termination codon caused by frameshift. Grey arrowheads indicate double strand break region by CRISPR/Cas9 and Red line indicate changed amino acid. A.A: amino acid PTC: Premature termination codon SNP: single nucleotide polymorphism (**d**) 2 homozygous offspring of Founder #2-4 showed hair loss in whole body on day 21 postpartum, and WT indicated wild type C57BL/6.

Sequencing was conducted for 3 expected founder mouse which were #1-4, #2-1 and #2-4 mouse. In #1-4 mice, -9bp deletion and -104, +2bp indel was observed (Figure 3c) and by the translation result only -3 and -34 amino acids were removed respectively with no frameshift causing premature termination codon(PTC) (Figure 3d). In #2-1 mice, 2bp from sgRNA#3 PAM site the single nucleotide polymorphism(SNP) was induced and -10bp deletion -11, +1bp indel and WT sequences were observed (Figure 3c). Translation result of #2-1 mice showed 174th glutamic acid changed to glycine and in indels allele PTC were induced with 23 amino acid changed at the end of the PTC (Figure 3d). In #2-4 mice, -4bp deletion and -114, +2bp indel and -150bp deletion were observed (Figure 3c) and each of the alleles were translated as PTC with 26 amino acid changed, PTC with 25 amino acid changed and just 50 amino acid deleted without any frameshift of PTC respectively (Figure 3d).

3.3 Germline transmission

To confirm the hereditary and phenotype that express in homozygous, germline transmission was conducted. In order to compare functional knockout by phenotype, #1-4 mouse which 34 amino acid deleted without frameshift or PTC and #2-4 mouse which were induced as PTC were crossed with wild type respectively. In line #1-4, 4 heterozygous mouse were obtained in F_1 level and final cross breeding to obtain homozygous was conducted by heterozygous and heterozygous mating. Eventually, 4 homozygous pups were obtained. In line #2-4, same cross breeding pathway was applied and 2 of homozygous was obtained. Gene inheritance was successfully

conducted according to the PCR, T7E1 and Sanger sequencing analysis. Homozygous that obtained from #2-4 Founder showed -112bp deletion, -4bp deletion and SNP allele and this appears to be different than #2-4 allele which were -114, +2bp indel and -4bp deletion. Even though founder mouse possesses the type which was found in homozygous mouse (-112bp del, -4bp del with SNP, -4 del), the gene analysis was conducted only by sequencing with cloning not by the deep sequencing so various type of mutation were not detected in founder mouse (Figure 4).

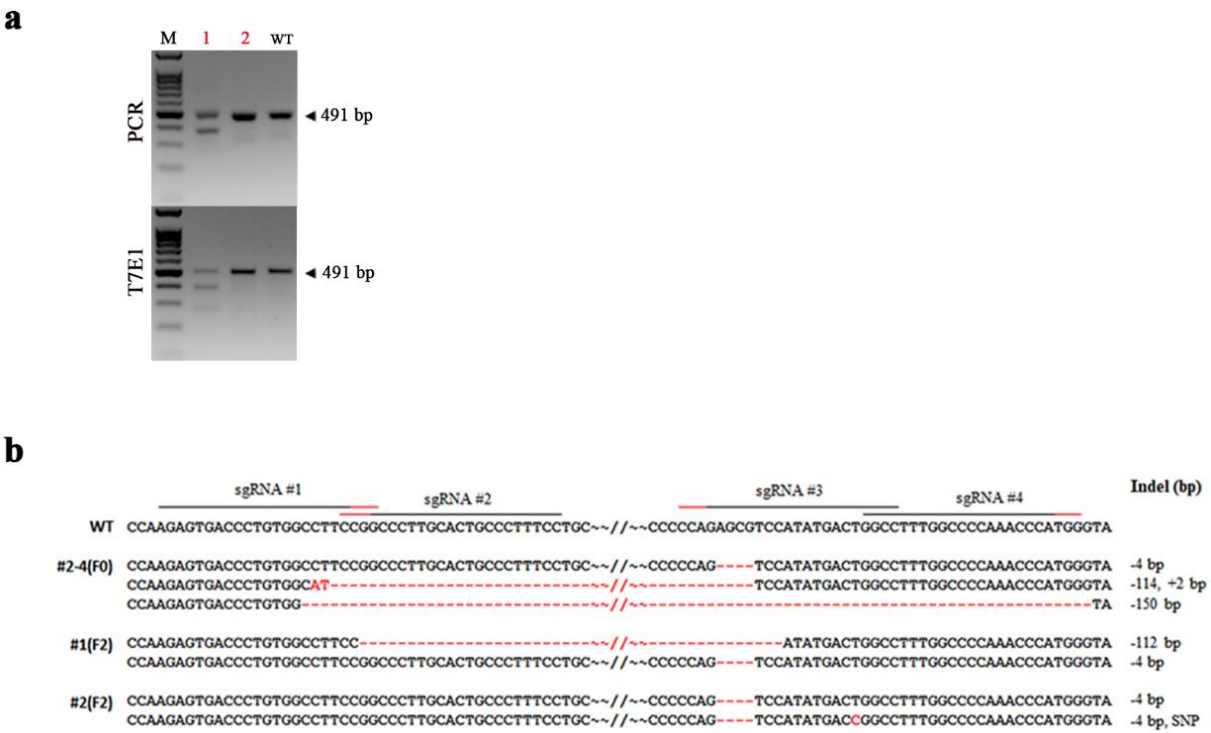

Figure 4. **Analysis of gene expression in line Founder #2-4. (a)** PCR and T7 endonuclease(T7E1) based analysis was conducted. Red letters indicate DNA cleaved pip. M: size marker, WT: wild type control. **(b)** Results of sequencing in each sgRNA binding sites. Sequences of 2 pups (#1 and #2) from #2-4 founder were compared. Red "-" and red letters indicate deleted and inserted nucleotides, respectively.

3.4 Hairless Phenotype

From second germline transmission which is possible to gain homozygous mouse phenotype was monitored every-day. On the 6 day after birth, fuzz starting to appear in homozygous mouse. The hair loss period was different by the mice but mostly on day 14 postpartum, local part of the rostral hair began to fall. From rostral to caudal side the hair was eliminated gradually and on day 21 postpartum, whole body exhibit alopecia phenotype (Figure 3e).

3. Discussion

CRISPR/Cas9 system is an efficient tool for developing DSB and consequential non-homologous end joining (NHEJ)-mediated KO. Using CRISPR/Cas9 system, generation of hairless mouse strain designated as *Hr*$^{-/-}$ mice was successfully conducted. Three different mutant form of founder mouse which are #1-4, #2-1, #2-4 was obtained. #1-4 line which has -3 amino acid and -34 amino acid deletion type without any frameshift of PTC showed no hairless phenotype even though some part of amino acid was deleted. #2-4 line which has PTC and -50 amino acid deletion type showed hairless phenotype in homozygous level. This result indicates nonsense mutation affect severe to gene expression.

Although the molecular mechanisms of hair loss is not completely understood[16], a number of *Hr* mutant mouse have been reported and *Hr*$^{-/-}$ mutant mouse exhibits hair loss after growth of the first hair coat and does not grow a second coat[17]. In #2-4 mice line which possesses homozygous nonsense mutation showed hairless phenotype pattern and this was identical as previous. These symptoms were different than barbering behavior (Dalila effect) which is an expression of dominance[18]. Barbering usually causes a local hair loss around muzzle or caudal side whereas Hr$^{-/-}$ hair loss extending from middle part of the forehead. Unlike body hair, vibrissae tend to exist until the late age and gradually pigment disappear and thickness becomes thin. On day 6 postpartum first hair comes up and on day 14 body hair begin to shed which completes on day 21. This complete hair loss mouse can be

utilized for *in vivo* imaging which is possible to detect clear fluorescence signal. Also, for dermatology research it reduces the effort for removing hair each time of experiment and which can cause scab formation due to bleeding.

There are many other genes related to hair functions. Particularly, Forkhead box protein N1 (*Foxn1*) gene is well known for alopecia phenotype. But *Foxn1* gene act as a master regulator of the thymic epithelial cells lineage development, differentiation resulting in fully function of thymus[19]. Therefore, *Foxn1*$^{-/+}$ expresses thymus enlargement and *Foxn1*$^{-/-}$ mutant mice expresses alopecia as well as athymia which could be premature lethal[20, 21]. Whereas also alopecia related gene *Hr,* mostly involved in hair growth and concomitantly participate in transcriptional corepressor of multiple nuclear receptors, including thyroid hormone receptor, the retinoic acid receptor-related orphan receptors and vitamin D receptors[22, 23]. Those immune related symptoms are useful for immune research but for research which simply needs hairless phenotype, it could affect the experiment result. Therefore, to utilize in various researches especially in *in vivo* imaging I selected less lethal gene to generate alopecia model. In a few studies, *Hr* mutant mouse were also reported as having abnormal immune system such as decrease in T cell number[24] and proliferation[25] as well as increase in macrophage cell number[26]. However, Hr$^{-/-}$ generated mouse in this study showed no severe immune abnormality externally.

For more practical usage not only external appearance further experiment is

needed. Histopathological study about hair follicle and immune population analysis were not conducted in $Hr^{-/-}$. Also, direct fluorescence protein delivery using such as viruses to $Hr^{-/-}$ can clearly present *in vivo* imaging possibilities.

In conclusion, we generated hairless mouse in C57BL/6 strain using CRISPR/Cas9. These hairless mouse will enable not only dermatological research but also *in vivo* imaging without variable affecting factor.

Chapter II

Whole Genome Sequencing Of Genome Modified mice generated with *Campylobacter jejuni* Cas9 reveals High Specificity of CRISPR/Cas9

1. Introduction

Gene engineering is a valuable technology in generating animal models for human disease and elucidating molecular mechanism of genetic diseases. Traditionally, knock out animals, especially mice, are produced by germ-line transmission of chimeric animals created based on the genetically engineered embryonic stem cells[27]. Targeted gene inactivation, replacement, addition has been achieved by homologous recombination. However, low efficiency of homologous recombination in mammalian cells has limited the utility of this approach. Recently, programmable nuclease including Zinc finger nuclease, transcription activator-like effectors and clustered regularly interspaced short palindromic repeat (CRISPR)/CRISPR associated protein were dramatically improved the efficiency of mammalian genome editing[1].

The CRISPR/Cas9 is RNA mediated adaptive defense system for viruses and plasmids[28], and it is efficient system for gene manipulation in eukaryotic cells[29]. Especially, the *Streptococcus pyogenes* Cas9 (SpCas9) is widely used, and it mediated gene targeting with single guide RNA (sgRNA) or pair of crRNA and tracrRNA with adequate protospacer adjacent motif (PAM)[12]. CRISPR/Cas9 system shows high activity and recognition fidelity, so it used for many field of research such as seed development, animal model generation and therapeutic approach[30]. CRISPR/Cas9 mediate double strand break (DSB) on target sites, and DSB induce repair process such as non-homologous end joining (NHEJ) or homologous direct repair (HDR).

NHEJ is error-prone repair and induce insertion and deletion (indel), thus it could be applicable for inducing targeted deletion or disruption of gene function. HDR is precise repair pathway, and is useful for inducing specific point mutation or exogenous DNA insertion exogenous by homologous recombination[31].

Even though, SpCas9 showed high efficiency of gene editing, there is still limitation of genome recognition with "NGG" PAM sequence. Several CRISPR/Cas9 orthologues such as *Staphylococcus aureus* Cas9 (SaCas9, PAM: 5'-NNGRRT-3'), *Lachnospiraceae* Cpf1 (LbCpf1, PAM: 5'-TTTV-3') and *Acidaminococcus* Cpf1 (AsCpf1, PAM: 5'-TTTV-3') exhibit high efficiency of targeted mutant mice generation[32-34]. In addition, they presented several advantages in comparing SpCas9. SaCas9 is sized about 3.16 kb, and it could be packed in adeno-associated virus (AAV) for in vivo gene editing[35]. Cpf1 develop 5' overhang DNA cleavage, and it could be helpful for HDR mediated gene editing[36].

Recently, *Campylobacter jejuni* Cas9 (CjCas9) was reported as type II-C CRISPR/Cas9 orthologue[37, 38]. CjCas9 gene is sized 2.95 kb with 984 amino acid, allowing it to be packaged into a single AAV vector with its sgRNA. Thereby, CjCas9 has potential to be utilized for *in vivo* gene editing[39]. Even though Fonfara et al.[37] suggested 5'-NNNNACA-3' as PAM sequence, but other group newly reported 5'-NNNVRYM-3', 5'-NNNNACAC-3' or 5'-NNNNRYAC-3' as specific PAM sequence[39, 40]. The targeting efficiency of CjCas9 was studied in cells and expected with low DNA cleavage activity[40, 41], but was analyzed only for NHEJ mediated

indel formation, not in zygote and HDR mediated precise editing. Additionally, there was recent report about off-target effect in SpCas9. Whole-genome sequencing (WGS)-based identification of off-target mutations showed unexpected mutations caused by CRISPR-Cas9 which were intended to correct mutation of *Pde6b* gene in blind rd1 mice through embryo genome editing[42]. On the other hand, the first human embryo gene correction study via CRISPR-Cas9 showed no off-target mutations[43]. Although these two results showed contrasting results, both utilized Cas9 derived from *Streptococcuus Pyogene* (SpCas9). Because of its simple protospacer adjacent motif (PAM) sequence, 5'-NGG-3', genome editing with SpCas9 is robust. However, its simple PAM sequence can result in more unwanted off-target sites. On the other hand, CjCas9 has long PAM sequence 5'-NNNNACAC-3' or 5'-NNNNRYAC-3' [39, 40], results in less robust target sites when compared to SpCas9, however this may also results in higher specificity. In this study, we generated knockout mice using CjCas9 and investigated gene editing efficiency and specificity of CjCas9. Next-generation sequencing (NGS)-based targeted deep sequencing revealed high efficiency of NHEJ- mediated gene targeting and whole-genome sequencing (WGS)-based unbiased off-target analysis revealed high specificity of CjCas9.

2. Materials and Method

2.1 Animals

C57BL/6 mice were obtained from Koatech (Pyeongtaek, Korea). All mice were maintained in individual ventilated cages and given access to food and water *ad libitum*. This study was approved by the Institutional Animal Care and Use Committees of Seoul National University (SNU-170308-13, SNU-170308-14 and SNU-170308-15) and was conducted in accordance with approved guidelines.

2.2 Preparation of CjCas9 mRNA and sgRNA

The CMV-CjCas9-pA plasmid was obtained from Toolgen Inc (Korea). Briefly, pCMV-CjCas9-pA was linearized by XbaI enzyme cutting and DNA was collected by centrifugation after -20 ºC for 15 min incubation. In vitro capped transcription and polyadenylation tailing were conducted with mMESSAGE mMACHINE T7 ultra kit (Thermo Fisher Scientific, Waltham, MA, USA) according to introduction. Brief structure of pCMV-CjCas9-pA was shown in Figure 5. sgRNAs for each gene were designed according to its PAM sequence (NNNNRYAC or NNNNACAC)[39], and screened off-target sequence by the cas-offinder (http://www.rgenome.net/cas-offinder). sgRNAs synthesized using an in vitro RNA-synthesis kit (Thermo Fisher Scientific, Waltham, MA, USA) following PCR amplification. sgRNA sequences were listed in Table 4. ssODNs were designed and synthesized with commercial service (IDT, San Jose, CA, USA).

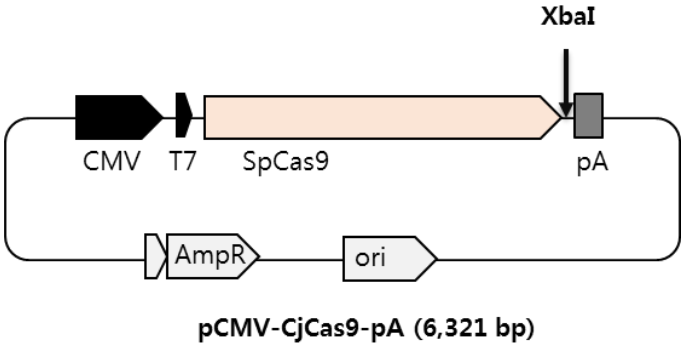

Figure 5. Structure of pCMV-CjCas9-pA. Plasmid include CMV enhancer and promoter (584 bp), T7 promoter (19 bp), CjCas9 gene (2,961 bp) and bovine growth hormone polyadenylation signal sequence (225 bp).

Table 4. sgRNA sequences used in this study

Target gene	Exon	sgRNA binding sequence	PAM
Tyr	1	AGCACTGGCAGGTCCTATTA	TAAAACAC
	1	AGCCCCCAAGCAGTGTGTCC	CTTGACAC
Foxn1	2	AGAGAGGACACCCTCACTGC	CCCCACAC
	2	CCAGACGGCCATGGCACTTG	ATGGACAC

2.3 Embryo microinjection

Superovulation was conducted by injection of pregnant mare's serum gonadotropin (Prospec Bio, East Brunswick, NJ, USA) and human chorionic gonadotropin (Prospec) for 46~48 hours interval into C57BL/6 female mice, and they were mated with sperm donor C57BL/6 males. On following day, the embryos were collected in M2 medium (MTI-Global stem, Rockville, MD, USA), and incubated for 3 hours in KSOM medium (Merk Millipore, Billerica, MA, USA). Normal embryos with two pronuclei were selected, and microinjection was conducted with a micromanipulator (Eppendorf, Hamburg, Germany). Briefly, 50ng/μL of CjCas9 mRNA, 10 ng/μL of sgRNA, or 20ng/μL of ssODN were mixed, and microinjected into pronucleus. Embryos were cultured to the 2-cell stage, and transferred to surrogated female or culturing until the blastocyst stage for genotyping.

2.4 Genotyping and sequencing

DNA was extracted from morula embryos or blastocysts and the tail of pups. Single embryos were transferred to 150-μL tubes filled with 20 μL distilled water by mouth pipette and subsequently used as templates for PCR analysis following three rounds of freezing/thawing and denaturation at 95ºC for 15 min. DNA extraction from tails was conducted using a gDNA-extraction kit (Intron Bio, Kyungki-Do, Korea). After PCR reaction, amplicons were used for T7E1 analysis (NEB, Ipswich, MA, USA) or used for TA cloning and Sanger sequencing (Cosmo Genetech, Seoul, Korea). All primer for genotyping was listed in supplementary Table 5.

Table 5. Primer sequences for genotyping used in this study

Target gene	Primer	Product size (bp)	Annealing Tm (ºC)
Tyr	F: 5'-TGATGTAAGAAGGGGAGTGG-3'	693	60
	R: 5'-AGGAGGAGAAGAAGGATGC-3'		
Foxn1	F: 5'-AGAAGGGCCAAGTCACAG-3'	759	60
	R: 5'-AGGAGAGAGGAGGTGGAAG-3'		

2.5 In silico design of Off-target sites

Potential off-target sites were designed in silico using on-line tool (www.rgenome.net). Up to 3 bp mismatches were considered as off-target sites.

2.6 Targeted deep sequencing

On-target and potential off-target sites were amplified from genomic DNA using Phusion polymerase taq (New England BioLabs). The PCR products were then deep sequenced using an Illumina MiSeq. A list of primers used can be found in Table 6. Indels around the site 3 bp upstream of the PAM sequence were counted as true mutations from Cas9 activity.

Table 6. List of primers used for targeted deep sequencing

Target	Forward (5' to 3')	Reverse (5' to 3')
Foxn1 On 1	ACACTCTTTCCCTACACGACGCTCTTCCGATCTAGATTCTCTATTCTGTCTGC	GTGACTGGAGTTCAGACGTGTGCTCTTCCGATCTAGGATACTTTTCTGAAGGAG
Foxn1 On 2	ACACTCTTTCCCTACACGACGCTCTTCCGATCTTGGCTTTGGCTTTGAGGAGG	GTGACTGGAGTTCAGACGTGTGCTCTTCCGATCTTGGGAAGCTAGGCAGGAAGG
Foxn1 Off 1-1	ACACTCTTTCCCTACACGACGCTCTTCCGATCTTGAATGACAGGAAGCTGCTC	GTGACTGGAGTTCAGACGTGTGCTCTTCCGATCTTTGCTATAGAATGACCAGCG
Foxn1 Off 1-2	ACACTCTTTCCCTACACGACGCTCTTCCGATCTTTGGTGACCTTGATGGACAC	GTGACTGGAGTTCAGACGTGTGCTCTTCCGATCTCAAGTTGTCCTCTTTGAGTG
Foxn1 Off 1-3	ACACTCTTTCCCTACACGACGCTCTTCCGATCTTGTGCATGTGTCCTTGTCTG	GTGACTGGAGTTCAGACGTGTGCTCTTCCGATCTTCTATGGCTTGCTTGCTTCC
Foxn1 Off 1-4	ACACTCTTTCCCTACACGACGCTCTTCCGATCTTCCAGGCATTTCAGGTGAGG	GTGACTGGAGTTCAGACGTGTGCTCTTCCGATCTGTGTTGGGAACCCTCTTGG
Foxn1 Off 1-5	ACACTCTTTCCCTACACGACGCTCTTCCGATCTACCACCAGACACATCCTCCA	GTGACTGGAGTTCAGACGTGTGCTCTTCCGATCTGCTGCCCACATTATTTCTGC
Tyr On 1	ACACTCTTTCCCTACACGACGCTCTTCCGATCTCAGGATATCCTTCTGTCCAG	GTGACTGGAGTTCAGACGTGTGCTCTTCCGATCTAGACTGAGCTGATAGTATG
Tyr On 2	ACACTCTTTCCCTACACGACGCTCTTCCGATCTATGAACAATGGGTCAACACC	GTGACTGGAGTTCAGACGTGTGCTCTTCCGATCTCAAGAAAAGTCTGTGCCAAG
Tyr1 Off 1-1	ACACTCTTTCCCTACACGACGCTCTTCCGATCTAATACCTACCCATCCATGT	GTGACTGGAGTTCAGACGTGTGCTCTTCCGATCTGGAGCAGAGATTATAACCTT
Tyr1 Off 2-1	ACACTCTTTCCCTACACGACGCTCTTCCGATCTAAGCCACCTGGCTAAGACTG	GTGACTGGAGTTCAGACGTGTGCTCTTCCGATCTAGCCAGTCTTGAGGAGTAAG

2.7 Whole genome sequencing

Whole genome sequencing and bioinformatics analysis was conducted by theragenetex (Suwon-si, Gyeonggi-do, Republic of Korea).

3. Results

3.1 High cleavage activity of CjCas9 in knock out mice generation

To assess the gene targeting efficiency of CjCas9, we selected Tyrosine (*Tyr*) gene as target and designed 2 sgRNAs with 22 nucleotide (nt) sized and 5'-NNNNACAC-3' PAM in exon 1. Distance between each sgRNA was 266 bps, and located in same anti-sense strand (Figure 6a). Next, I microinjected CjCas9 mRNA and sgRNAs into embryos, and conducted PCR and T7E1 based genotyping. Of total 9 embryos, 9 embryos were successfully genotyped, and they showed high cleavage efficiency of 100 % (8/8), and it was higher than our expectation (Figure 6b and Table 7). After confirming high targeting efficiency of CjCas9, I transferred 25 microinjected embryos into surrogate dam and obtained 4 pups, and all produced pups were found to be founder with albino phenotype (Figure 6c, 6e).

Table 7. Summary of CjCas9 mediated KO mice generation

Gene	Type	No of injected embryo	No. of 2 cell stage embryo (%)	No. of BL (%)	No. of transferred embryos	No. of offsprings (%)	Targeting efficiency (%) (No. of mutant/total blastocysts or offsprings)
Tyr	KO	34	NA	9(37.9)	NA	NA	100 (8/8)
					25	4 (16%)	100 (4/4)
Foxn1	KO	39	NA	13(50)	NA	NA	81.8 (9/11)
					50	13 (26%)	38.4 (5/13)

a

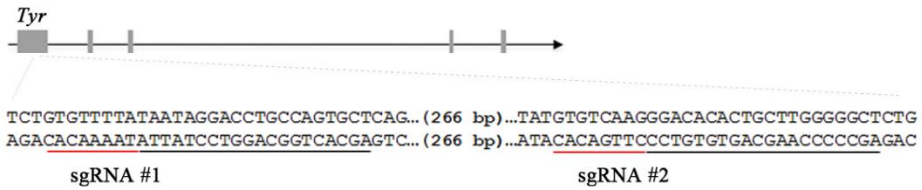

b

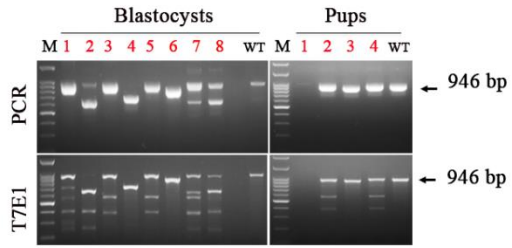

c

d

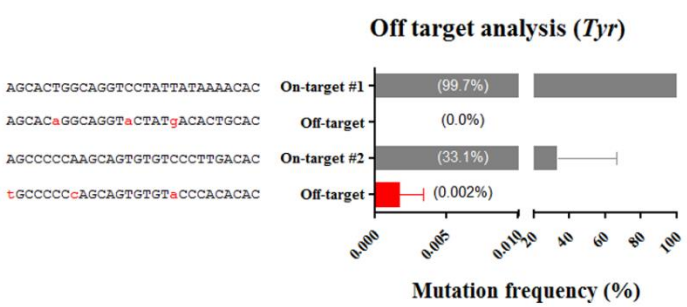

e

Tyr mutant pup (15 days old)

Figure 6. *Tyr* KO mice generation with CjCas9. (a) Schematic represent target site for gene targeting. Two sgRNAs with 22 nucleotide sequence of binding site (black line) were used, and red line indicate PAM sequence (5'-NNNNACAC-3'). These two sgRNAs were located in exon 1 of Tyrosinase gene.Gray box indicate exon. (**b**) PCR and T7 endonuclease (T7E1) based analysis for blastocysts and produced pups was conducted. Both in Blastocyst and Pups showed 100% of DNA cleavage efficiency. Red letters indicate DNA cleaved blastocyst or pup. M: size marker, WT: wild type control. (**c**) Results of sequencing (#1 founder) and targeted deep sequencing assay (#2, 3, and #4 founders) in each sgRNA binding sites. Red "-" and red letters indicate deleted and inserted nucleotides, respectively. (**d**) Analysis of off-target effects of CjCas9 in the 2 sgRNA site of *Tyr* gene. Less than three base pair mismatch sites of each sgRNA were selected, and PCR based deep sequencing was conducted with DNAs from founder pups. Exist of indel around sgRNA target site or off-target site was considered as CjCas9 mediated mutation. Data was presented as mean ± standard error in the mean (SEM). (**d**) All produced pups showed white hair in whole body, and WT indicated wild type C57BL/6.

To investigate the reproducibility of cleavage activity of CjCas9, I selected Forkhead box protein N1 (*Foxn1*) gene as target. Similar with *Tyr* targeting, dual sgRNAs with 5'NNNNACAC-3' PAM were designed, and obtained blastocysts and pups after microinjection and embryo transfer (Figure 7a). PCR and T7E1 based genotyping with blastocysts results exhibited 81.8% (9/11) of cleavage efficiency, and it was similar with targeting rate in *Tyr*. In addition, 5 from 13 produced pups (38.4%) were found to be showing indel, and it was lower cleavage efficiency than showing in blastocysts (Figure 7b). In addition, founder pups did not exhibit alopecia phenotype.

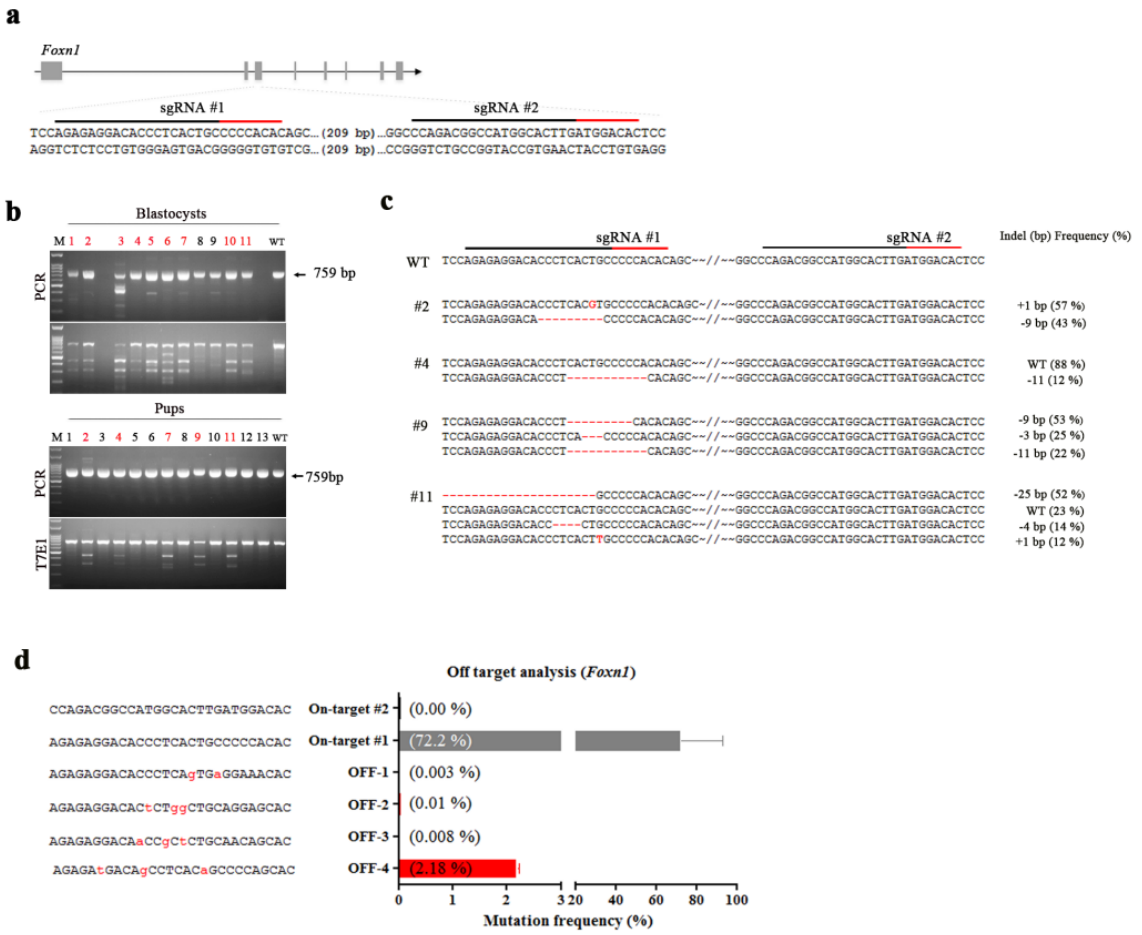
a
Foxn1
sgRNA #1
sgRNA #2
TCCAGAGAGGACACCCTCACTGCCCCCACACAGC...(209 bp)...GGCCCAGACGGCCATGGCACTTGATGGACACTCC
AGGTCTCTCCTGTGGGAGTGACGGGGGTGTGTCG...(209 bp)...CCGGGTCTGCCGGTACCGTGAACTACCTGTGAGG
b
Blastocysts
M 1 2 3 4 5 6 7 8 9 10 11 WT
PCR
759 bp
Pups
M 1 2 3 4 5 6 7 8 9 10 11 12 13 WT
PCR
759bp
T7E1
c
sgRNA #1
sgRNA #2
Indel (bp) Frequency (%)
WT TCCAGAGAGGACACCCTCACTGCCCCCACACAGC~~//~~GGCCCAGACGGCCATGGCACTTGATGGACACTCC
#2 TCCAGAGAGGACACCCTCACGTGCCCCCACACAGC~~//~~GGCCCAGACGGCCATGGCACTTGATGGACACTCC +1 bp (57 %)
TCCAGAGAGGACA---------CCCCCACACAGC~~//~~GGCCCAGACGGCCATGGCACTTGATGGACACTCC -9 bp (43 %)
#4 TCCAGAGAGGACACCCTCACTGCCCCCACACAGC~~//~~GGCCCAGACGGCCATGGCACTTGATGGACACTCC WT (88 %)
TCCAGAGAGGACACCCT----------CACAGC~~//~~GGCCCAGACGGCCATGGCACTTGATGGACACTCC -11 (12 %)
#9 TCCAGAGAGGACACCCT---------CACACAGC~~//~~GGCCCAGACGGCCATGGCACTTGATGGACACTCC -9 bp (53 %)
TCCAGAGAGGACACCCTCA---CCCCCACACAGC~~//~~GGCCCAGACGGCCATGGCACTTGATGGACACTCC -3 bp (25 %)
TCCAGAGAGGACACCCT----------CACAGC~~//~~GGCCCAGACGGCCATGGCACTTGATGGACACTCC -11 bp (22 %)
#11 ----------GCCCCCACACAGC~~//~~GGCCCAGACGGCCATGGCACTTGATGGACACTCC -25 bp (52 %)
TCCAGAGAGGACACCCTCACTGCCCCCACACAGC~~//~~GGCCCAGACGGCCATGGCACTTGATGGACACTCC WT (23 %)
TCCAGAGAGGACACC----CTGCCCCCACACAGC~~//~~GGCCCAGACGGCCATGGCACTTGATGGACACTCC -4 bp (14 %)
TCCAGAGAGGACACCCTCACTTGCCCCCACACAGC~~//~~GGCCCAGACGGCCATGGCACTTGATGGACACTCC +1 bp (12 %)
d
Off target analysis (Foxn1)
CCAGACGGCCATGGCACTTGATGGACAC On-target #2 (0.00 %)
AGAGAGGACACCCTCACTGCCCCCACAC On-target #1 (72.2 %)
AGAGAGGACACCCTCAgTGaGGAAACAC OFF-1 (0.003 %)
AGAGAGGACACtCTggCTGCAGGAGCAC OFF-2 (0.01 %)
AGAGAGGACAaCCgCtCTGCAACAGCAC OFF-3 (0.008 %)
AGAGAtGACAgCCTCACaGCCCCAGCAC OFF-4 (2.18 %)
0 1 2 3 20 40 60 80 100
Mutation frequency (%)

Figure 7. *Foxn1* KO mice generation with CjCas9. (a) Schematic represent target site for gene targeting. Two sgRNAs with 22 nucleotide sequence of binding site (black line) were designed in exon 3 of *Foxn1* gene, and red line indicate PAM sequence (5'-NNNNRYAC-3'). Gray box indicate exon. (**b**) PCR and T7E1 assay for blastocysts and produced pups was conducted. DNA cleavage efficiency showed 81% (9/11) and 38% (5/13) in blastocyst and pup respectively. Red letters indicate cleaved blastocyst or pup. M: size marker, WT: wild type control. (**c**) Targeted deep sequencing assay in each sgRNA target sites. Red "-" and red letters indicate deleted and inserted nucleotides, respectively. (**d**) Analysis of off-target effects of CjCas9 in the 2 sgRNA site of *Foxn1* gene. Less than 3 base pair mismatch site were selected, and PCR based deep sequencing was conducted with DNAs from founder pups. Exist of indel around sgRNA target site or off-target site was considered as CjCas9 mediated mutation. Data was presented as mean $\pm$ standard error in the mean (SEM).

3.2 Off-target Analysis showed high specificity

Targeted deep sequencing showed mutations in both allele (~100% indel frequency; Figure 6c, 7c). Functional Tyr protein knockout from CjCas9-mediated gene knockout was confirmed by detecting albino in Tyr knockout founders (Figure 6e). To find out potential off-target sites, I predicted off-target sites up to 3 bp mismatches *in silico* (Table 8).

Table 8. Off target sites for CjCas9 targeted *Try* and *Foxn1* genes.

Target gene		Target (mismatches) PAM	Chr	Position	Direction	Mismatches	Gene
Tyr	On-target #1	AGCACTGGCAGGTCCTATTATAAAACAC[a]	7	87493076	+	0	Tyr (Exon)
	OFF-1	AGCACa[b]GGCAGGTa[b]CTATg[b]ACACTGCAC	1	40875720	-	3	Intergenic region
	On-target #2	AGCCCCCAAGCAGTGTGTCCCTTGACAC	7	87492776	+	0	Tyr (Exon)
	OFF-1	tGCCCCCcAGCAGTGTGTaCCCACACAC	7	30058274	-	3	Zfp62 (Intron)
Fxon 1	On-target #1	AGAGAGGACACCCTCACTGCCCCCACAC	11	78371343	-	0	Foxn1 (Exon)
	OFF-1	AGAGAGGACACCCTCAgTGaGGAAACAC	3	84010554	-	2	D930015E06Rik (Intron)
	OFF-2	AGAGAGGACACtCTggCTGCAGGAGCAC	5	142839030	+	3	Intergenic region
	OFF-3	AGAGAGGACAaCCgCtCTGCAACAGCAC	1	89639411	-	3	Agap1 (Intron)
	OFF-4	AGAGAtGACAgCCTCACaGCCCCAGCAC	6	88449421	+	3	Intergenic region
	OFF-5	AGgGAGGACACCCTCACaGaGAAAGCAC	14	55481306	+	3	Dhrs4 (Intron)

[a]PAM sequence
[b]mismatch sequences

Consistent with targeted deep sequencing, I detected the *Tyr* and *Foxn1* mutant alleles in Tyr-2, Tyr-4 and Foxn1-2, Foxn1-9, respectively (Figure 6c, 7c). Of all potential off-target sites found by in silico-based online search tool (Cas-OFFinder; www.rgenome.net), I found a small changes in Foxn1-Cj1-Off #1 sites. This site contained repeated sequences, suggesting that indels found at this site was caused by sequencing errors during alignment rather than Cas9-induced off-target DNA cleavage. Targeted deep sequencing of these potential off-target sites revealed high specificity of Tyr and Foxn1 targeting sgRNAs (Figure 6d, 7d).

3.3 WGS based bioinformatics analysis revealed different off-target rate by the control mice

Having achieved knockout colonies by using CjCas9, I then investigated target specificities in whole genome level. I selected 2 samples from Tyr and Foxn1 mutated founders (Tyr-2, Tyr-4, Foxn1-2 and Foxn1-9), 2 WT controls from same vendors where I ordered female mice to perform microinjections (WT1, WT2), 2 internal negative controls from Foxn1-targeting dual sgRNAs and mRNA encoding CjCas9 treated founders, yet showed WT genotypes (Foxn1-12 and Foxn1-13). To identify any potential off-target indel or SNVs caused by CjCas9, WGS was performed for these samples at a sufficient depth (x20-30) to detect more than 95% of heterozygous variants. I applied multiple computational methods to detect small indels, the hallmark of Cas9-induced damage or SNVs. I extended our analysis to the remainder of the genome. Variant concordance check with each of the individual mice was conducted. Variant concordance of genomic allele showed ≤70% match when it compared

including non-litter mate (WT1, WT2) and litter mate(Tyr-2, Tyr-4, Foxn1-2, Foxn1-9, Foxn1-12 and Foxn1-13) whereas when only including litter mate(Tyr-2, Tyr-4, Foxn1-2, Foxn1-9, Foxn1-12 and Foxn1-13) showed higher concordance (74-76%) (Figure 8a). Identified indels and SNVs from each sample were aligned to compare indels and SNVs among different groups (Figure 8b). This analysis essentially separated all samples to two groups; 1. WT group and 2 sgRNAs/CjCas9 treated groups (Tyr-2, Tyr-4, Foxn1-2, Foxn1-9, Foxn1-12 and Foxn1-13) by indel and SNV similarities (Figure 8b, c).

a

	Vendor WT		CjCas9 treated KO		CjCas9 treated littermate WT		CjCas9 treated KO	
	B6-WT-1	B6-WT-2	Foxn1-2	Foxn1-9	Foxn1-12	Foxn1-13	Tyr-2	Tyr-4
B6-WT-1		69.60%	66.49%	65.92%	66.32%	66.26%	66.82%	66.00%
B6-WT-2			67.05%	66.65%	66.96%	66.80%	67.34%	66.63%
Foxn1-2				74.66%	75.40%	75.12%	76.01%	74.80%
Foxn1-9					74.22%	74.11%	74.86%	74.21%
Foxn1-12						75.45%	75.46%	75.26%
Foxn1-13							75.27%	75.09%
Tyr-2								75.21%
Tyr-4								

b

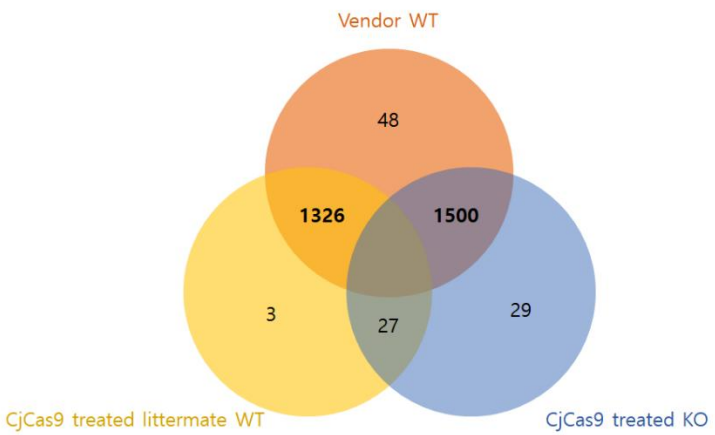

c

ID	SNP·InDel difference
B6-WT-1_vs_B6-WT-2	48
B6-WT-1_vs_Foxn1-12	1,372
B6-WT-1_vs_Foxn1-13	1,362
B6-WT-1_vs_Foxn1-2	1,603
B6-WT-1_vs_Foxn1-9	1,585
B6-WT-1_vs_Tyr-2	1,596
B6-WT-1_vs_Tyr-4	1,357
B6-WT-2_vs_Foxn1-12	1,292
B6-WT-2_vs_Foxn1-13	1,277
B6-WT-2_vs_Foxn1-2	1,527
B6-WT-2_vs_Foxn1-9	1,523
B6-WT-2_vs_Tyr-2	1,525
B6-WT-2_vs_Tyr-4	1,283
Foxn1-12_vs_Foxn1-13	3
Foxn1-12_vs_Foxn1-2	38
Foxn1-12_vs_Foxn1-9	38
Foxn1-12_vs_Tyr-2	37
Foxn1-12_vs_Tyr-4	3
Foxn1-13_vs_Foxn1-2	45
Foxn1-13_vs_Foxn1-9	25
Foxn1-13_vs_Tyr-2	29
Foxn1-13_vs_Tyr-4	0
Foxn1-2_vs_Foxn1-9	47
Foxn1-2_vs_Tyr-2	58
Foxn1-2_vs_Tyr-4	29
Foxn1-9_vs_Tyr-2	50
Foxn1-9_vs_Tyr-4	36
Tyr-2_vs_Tyr-4	10

Figure 8. ***Bioinformatics study with WGS*****. (a)** Variant concordance check. Vendor WT and CjCas9 treated mouse are not litter mate. Concordance showed higher when the sequences are aligned with same litter mate mouse whereas comparison with Vendor WT (non-littermate) showed lower concordance. This indicates even though all the mouse that were used in whole genome sequencing were from the same vendor yet they are not completely 'inbred'. *conditions of filteration 1) if genotype is Reference Homozygote (RefHom), selection of ratio of reference alleles depth more than 90% 2) if genotype is Heterozygote (Hetero), selection of ratio of reference alleles depth more than 40% and less than 60% 3) if genotype is Alternative Homozygote (AltHom), selection of ratio alteration alleles depth more than 90% 4) total depth more than 10 (**b**) Venn diagrams displays single nucleotide variations (SNVs) which could also represent off-targets. SNVs were detected by WGS data based bioinformatics analysis. Comparison between non-littermate (Vendor WT vs CjCas9 treated littermate WT and Vendor WT vs CjCas9 treated KO) revealed higher off-targets. Whereas comparison between littermate (CjCas9 treated littermate WT vs CjCas9 treated KO) revealed few off-targets. Since concordance were low in non-littermate comparison, this could also impact on wrong off-target counting in bioinformatics. Vendor WT: non-CjCas9 treated wild type (B6-WT-1 and B6-WT-2), CjCas9 treated WT: CjCas9 treated wild type (Foxn1-12 and Foxn1-13), CjCas9 treated KO: CjCas9 treated knockout (Tyr-2, Tyr-4, Foxn1-2 and Foxn1-9). SNV·InDel differences were calculated and mean values were displayed. (**c**) Summary of SNV·InDel differences between individual mice.

4. Discussion

Ever since CRISPR/Cas9 system have been used for genome engineering, CRISPR type II *Streptococcus pyogenes* Cas9 was most commonly used. Recently, novel CRISPR type II orthologue, *Campylobacter jejuni* Cas9 showed possibility for genome editing tool in *in vitro*. I extended CjCas9 efficacy test in *in vivo* with zygote and through mice generation and the result showed unexpected high cleavage efficiency and low off-target of CjCas9.

Previously, Ma E *et al.* reported that type II-C which includes CjCas9 are inefficient for genome editing because a limited dsDNA binding and unwinding activity and promiscuous guide RNA specificity[41]. Despite the uncertainty of CjCas9, advantage of small size Cas9 which can allow compact packaging such as in AAV kept us interested. So I generated mice with CjCas9 to confirm cleavage efficiency and off-target. I selected two genes, *Tyr* and *Foxn1*, for reproducibility. Briefly, *Tyr* gene is involved in melanin conversion[44] so mutation in this gene result in oculocutaneous albinism[45], and non-pathologic polymorphisms result in skin pigmentation variation[46]. *Foxn1* gene is mostly involved in thymic epithelial cells development, differentiation and functioning. So, mutation in this gene mostly result in immune system but also appears alopecia phenotype. Due to easily detectable phenotypes, *Tyr* and *Foxn1* genes were manipulated. Result of using CjCas9, both genes showed 38-100% NHEJ rate. This rate may be different by the genomic locus but it surely showed high DSB rate for genome engineering tool. When CRISPR/Cas9

system showed prospect for genome editing, high cleavage efficiency was the critical point. However, as time passes gene therapy are drawing attention and the ultimate goal for this is to applicate in human. Therefore, discovering not only high editing ability but also low off-target CRISPR orthologue is significant. Regard to this issues off-target analysis of generated mice mediated from CjCas9 was conducted and it showed significantly low (≤1.6%) off-target. This result is because CjCas9 possesses long PAM sequence 5'-NNNNACAC-3' or 5'-NNNNRYAC-3' [39, 40] which can be less robust target sites when compared to SpCas9, however results in higher specificity. Beside not only just off-target analysis I also conducted bioinformatics studies by aligning CjCas9 treated knockout WGS data with different wild type control sequence (non-litter mate wild type vs litter mate wild type). This is in line with recent WGS data from Schaefer *et al*., 2017 who showed CRISPR/Cas9-treated and separately obtained WT samples are essentially different[42]. Although our WT mice were obtained from the same vendor and supposedly 'inbred', both results from us and Schaefer *et al.,* 2017 suggests that WT samples are not *bona fide* inbred. Altogether, these results suggest that indel and SNVs in CRISPR/Cas9 treated groups when compared to WT groups are more likely resulted from different breeding not Cas9-induced.

In this study CjCas9 cleavage activity and off-target analysis were tested in *in vivo*. However, yet direct compare with SpCas9 and CjCas9 haven't proceeded. Although, there are many report about SpCas9 mediated genome editing, efficacies are different by the genomic locus. Thus, further study is needed with using sgRNAs which shares

both 5'-NGG-3' and 5'-NNNNRYAC-3' PAM sequence (e.g. 5'-NGGNRYAC-3' or 5'-NNGGRYAC-3') so that it could cut same locus by both CjCas9 and SpCas9. This will clearly present efficacy between SpCas9 and CjCas9 without any variable affecting factors.

Consequently, our studies demonstrate high efficient and accurate genome engineering in *in vivo* with novel orthologue CjCas9. I suggest this results can broaden the range of application for safe gene therapy as well as multigene related cancer modeling. Also, while our results are in line with Schaefer et al., regarding numerous indel or SNV mutations that are unrelated to CRISPR/Cas9, these mutations are highly likely derived from the wild-type controls that are derived from different breeding colony. Therefore, I strongly argue against the argument of 'unexpected mutations after CRISPR-Cas9 editing *in vivo*' from Schaefer et al.

Chapter III

In vivo Multiple Gene Targeting with *Campylobacter jejuni* cas9 for Pancreatic Cancer

1. Introduction

Pancreatic ductal adenocarcinoma (PDAC) is one of the most lethal cancer type, which have rapid degeneration and resistance to treatment. Since the symptoms are nearly imperceptible, disease eludes detection period which cause a 5-year survival rate of ~5%[47]. The exact causes of pancreatic cancer are not known but several risk factors includes smoking, nonhereditary chronic pancreatitis etc. [47]. Still, there is ongoing study about cell origin and general agreement is that pancreatic intraepithelial cells in duct is believed to be the common outset of PDAC[48]. Most frequently mutated genes shown in pancreatic cancer are *Kras, Ink4a, Tp53, Smad4, Brca2*[48, 49] and each of the gene goes along with the degree of pancreatic intraepithelial neoplasia(PanIN) which classified into PanIN-1, PanIN-2, PanIN-3 and PDAC respectively[50]. Pancreatic cancer model could provide opportunities for understanding of complex gene interaction with pathological progression and preclinical study but barely none of them are generated[51].

Generating practical cancer animal model is difficult because pancreatic cancer arises with multiplex gene mutations and most of the related genes are lethal which affects lower germline penetrance (<10%) compared to other cancers[52-55]. Few technical advances have been made in PDAC mouse models, and even the existing models are generated from PDAC established model such as $Kras^{LSL\text{-}G12D}$,$p53^{LSL\text{-}R172H}$ based gene editing[56]. Thus conventional methods are hardly applicable, time-consuming and laborious resulting in the current studies about pancreatic cancer to

be localized in *in vitro* level. So, new modeling method is needed to generate multiplex gene targeting for pancreatic cancer.

Recently discovered CRISPR/Cas9 is an adaptive defense system in prokaryote cells which emerged as a powerful and efficient tool for gene manipulation in eukaryotic cells[12, 28, 29]. Due to conventional animal modeling limitations, genome engineering with CRISPR mediated somatic gene targeting through viral or electroporation delivery are highly drawing attention and researches have been conducted in various organs including lung, liver, brain, retina, pancreas[39, 56-61].

Here I attempt to generate pancreatic cancer model in adult mice by in vivo gene targeting. I used adeno-associated virus (AAV) for gRNA, Cas9 and homology arm delivery. *Streptococcus pyogenes* cas9 (SpCas9) was used for gene targeting but owing to limited AAV packaging size, Cas9 and gRNAs are injected by separated virus. I considered this would somehow affect in efficiency, additional experiment injecting gRNA viruses into Cas9 overexpression transgenic mouse was conducted. During the study using SpCas9, novel orthologue *Campylobacter jejuni* cas9 (CjCas9) for genome editing was reported[39]. Since CjCas9 has smaller size cas9 than SpCas9 which gives advantages for compact and effective AAV packaging, I added group targeting genes using CjCas9 and compared the efficiency rate.

2. Materials and Method

2.1 Target gene sgRNAs preperation

In many of pancreatic cancer related genes, specific genes were selected including *Kras* gain of function and *Ink4a1 (CdKn2a-ex1β), Ink4a2 (CdKn2a-ex2), Tp53, Smad4, Brca2* loss of function. In Kras G12D Knock-in, sgRNA with 20bp binding sequences and 5'-NGG-3' PAM for SpCas9 and 22bp binding sequences and 5'-NNNVRYM-3', 5'-NNNNACAC-3' or 5'-NNNNRYAC-3' PAM were designed. In donor template homology arms were prepared and silent mutations were given to prevent from re-cutting by sgRNA.

For SpCas9, sgRNA sequences were same as previous report[61] and in case of CjCas9, sgRNA sequences were newly designed according to 22bp binding sequences and PAM. All sgRNA sequences were shown in Table 9. sgRNA evaluation was conducted by microinjecting pAAV-3sgRNAs into C57BL/6 embryos which were collected by superovulation.

Table 9. sgRNA target region.

Target gene	Orthologue	Mutant	Chr[*a]	Exon	sgRNA binding sequence	RE[*b]
Kras	SpCas9	KI[*c]	6	1	GTGGTTGGAGCTGACGGCGT (AGG) [*e]	Bbs1
Ink4a-1	SpCas9	KO[*d]	4	1	TGGTGAAGTTCGTGCGATCC (CGG)	Sap1
Ink4a-2	SpCas9	KO	4	2	GTGCGATATTTGCGTTCCGC (TGG)	BspM1
Tp53	SpCas9	KO	11	3	GACACTCGGAGGGCTTCACT (TGG)	Bbs1
Smad4	SpCas9	KO	18	2	GACAACCCGCTCATAGTGATA (TGG)	Sap1
Brca2	SpCas9	KO	5	3	TAGGACCGATAAGCCTCAAT (TGG)	BspM1
Kras-1	CjCas9	KI	6	1	CCACCAGCTCCAACCACCACAA (GTTTATAC)	N/A[*f]
Kras-2	CjCas9	KI	6	1	GTGGCGTAGGCAAGAGCGCCTT (GACGATAC)	N/A
Ink4a-2	CjCas9	KO	4	2	TAGTGGGGTCCTCGCAGTTCGA (ATCTGCAC)	N/A
Tp53	CjCas9	KO	11	3	CCCTCCGAGTGTCAGGAGCTCC (TGCAGCAC)	N/A
Smad4	CjCas9	KO	18	1	GTTTCACTTTCCCCACCTTGTC (TATGACAC)	N/A
Brca2	CjCas9	KO	5	4	CTCTTACTCTGCGGTGCACACA (GGCAGTAC)	N/A

[*a:] Chromosome
[*b:] Restriction enzyme
[*c:] Knock-in (gain of function)
[*d:] Knockout (loss of function)
[*e:] PAM sequence
[*f:] CjCas9 were synthesized so restriction enzymes are not applicable

2.2 Generation of SpCas9 overexpression mice

Superovulation was conducted by injection of pregnant mare's serum gonadotropin (Prospec Bio, East Brunswick, NJ, USA) and human chorionic gonadotropin (Prospec) for 48hour interval into C57BL/6 female mice followed by mating with sperm donor C57BL/6 males. On following day, the embryos were collected in M2 medium (MTI-Global stem, Rockville, MD, USA), and incubated in KSOM medium (Merk Millipore, Billerica, MA, USA). Then transposase and PB-pCAG-SpCas9/RFP-polyA vector was microinjected into 1-cell embryos with micromanipulator (Eppendorf, Hamburg, Germany). Briefly, transgene map is shown in Figure 10b. Embryos were cultured to the 2-cell stage, and transferred to surrogated ICR females which were mated with vasectomized ICR males. PCR based genotyping was conducted and SpCas9 expression was confirmed by detecting RFP signals in each organ.

2.3 Vector Preparation of AAV2-SpCas9 and AAV2-3sgRNAs

To clone AAV expression plasmid, pAAV-CMV (AAVpro® Helper Free System, Takara Bio Inc., Japan) was used with minor modification. For multiple sgRNA targeting, 3 sets of U6 promoter-sgRNA scaffold packaged with AAV Inverted terminal repeats (ITRs) were synthesized (Integrated Device Technology, Inc., San Jose, CA, USA.) and cloned into pAAV-CMV. Due to pAAV-CMV contains *sap1* restriction enzyme (RE) site which overlap with sgRNA cloning RE, so additional infusion cloning was conducted for elimination. To put each sgRNAs in AAV plasmid(pAAV-3sgRNA), 3sgRNAs were selected for SpCas9 mediated depending

on stage of each gene expression and enzyme site were added on 5'-, 3'- end of sgRNAs respectively as preciously described[62]. Then golden gate cloning was used to put each sgRNAs into pAAV-3sgRNA backbone (Figure 9). Successful cloning was identified by RE cutting whereas in CjCas9, 3sgRNA sets were synthesized all together so restriction enzyme site for sgRNAs were unnecessary.

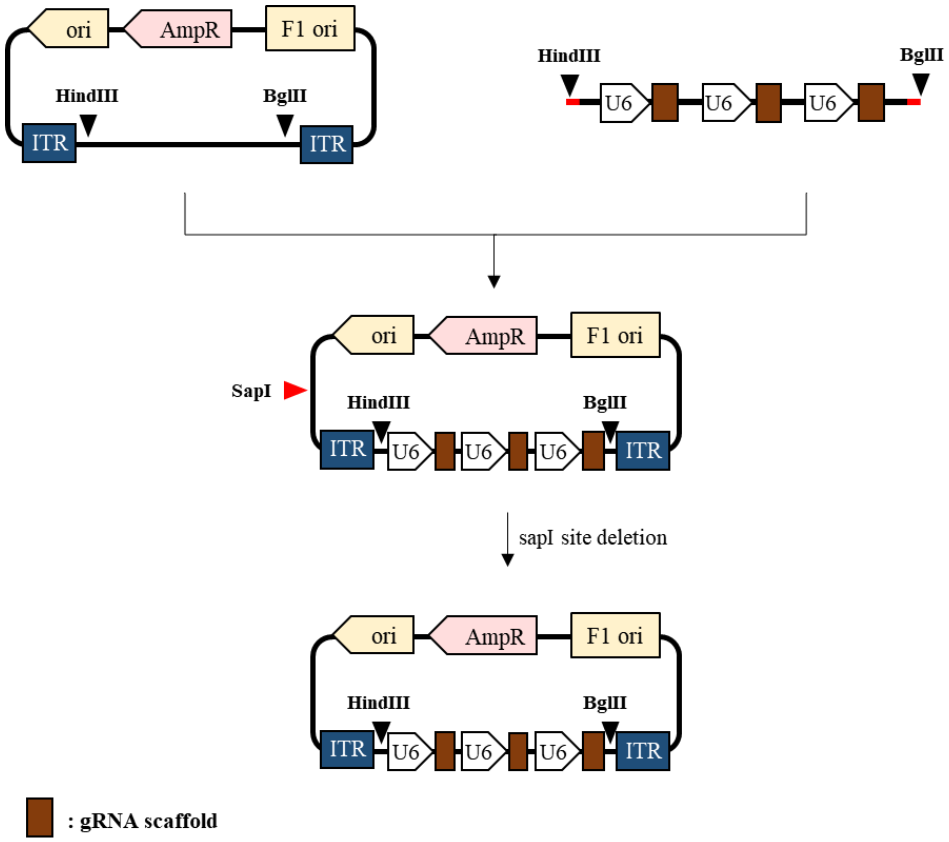

Figure 9. pAAV-3sgRNA modification strategy.

2.4 AAV preparation

AAV preparation was followed as AAVpro™ helper free system (Takara, Kusatsu, Shiga, Japan). Plasmid that expresses the Rep and Cap genes of AAV2(pRC-mi342) and adenovirus E2A, E4 and VA (pHelper) vectors were used intact and pAAV-CMV which is available to contain gene of interest(GOI) was modified by the target. Detail GOI combinations are shown in Fig. 1A. Tri co-transfection was conducted by using CalPhos™ Mammalian Transfection Kit (Takara, Kusatsu, Shiga, Japan) into HEK293T cells in 150mm cell culture dish. After 2 to 3 hours, medium was changed with culture medium containing 2% FBS. AAV2-producing cells were collected 4days after transfection and by using AAVpro™ Extraction solution (Takara, Kusatsu, Shiga, Japan) viruses were extracted. Virus titer was measured by qPCR by using AAVpro Titration Kit (Takara, Kusatsu, Shiga, Japan) and primers were designed at inverted terminal repeats (ITR) region.

2.5 AAV injection into pancreas

C57BL/6 (B6) and FVB from Koatech (Eumsung, Korea) and C57BL/6-TgTn (pb-Cag-spCas9/RFP) (PB-Cas9) were used for in vivo AAV injection and both were ranged between 4~6 weeks of age. In wild type B6 mice, AAV2-spCas9 and 2 sets of AAV2-3sgRNAs were co-injected in 7 mice (test group) and saline were injected in 5 mice (control group). In PB-cas9 mice, only 2 sets of AAV2-3sgRNAs were injected in 9 mice and saline in 5 mice. In FVB mice, 2 sets of AAV2-CjCas9-3sgRNAs were injected in 13 mice. Brief experimental design is shown in Figure 10a.

Injected AAV2 SpCas9 viral particle was 2.6 X 10^{10} and AAV2-sgRNAs was 1.29 X 10^{10}. All in one vector which contains AAV2 CjCas9 and sgRNAs and AAV2 GFP were both injected in 1.29 X 10^{10} (Table 10). Final injection volume was 200μl and each virus mixture was diluted with saline and added 0.5% trypan blue. AAV injection was conducted as previously reported method with minor modification [56]. Briefly, after anesthetizing and dissection from lower abdomen to diaphragm, duodenum was gently pulled over and was covered with wet gauze for preventing dry, and AAV was injected into sphincter of oddi under microscope with 30-gauge needle.

This study was approved by the Institutional Animal Care and Use Committees of Seoul National University (SNU-160913-2) and was conducted in accordance with approved guidelines.

Table 10. Summary of in vivo gene targeting group

Group	Strain.	Sex.		N	Component	Virus Titer (Vg/ML)	No. of Virus particle
Group1	C57BL/6	Male	AAV Treated	7	AAV-SpCas9	2×10^{12}	2.6×10^{10}
					AAV-Ink4a1-Ink4a2-Kras-Kras HA	1.5×10^{12}	1.29×10^{10}
					AAV-Tp53-Smad4-Brca2	1.7×10^{12}	1.29×10^{10}
			Control	5	Saline	-	-
Group2	C57BL/6-Cas9 TG	Male	AAV Treated	9	AAV-Ink4a1-Ink4a2-Kras-Kras HA	1.5×10^{12}	1.29×10^{10}
					AAV-Tp53-Smad4-Brca2	1.7×10^{12}	1.29×10^{10}
			Control	5	Saline	-	-
Group3	FVB	Male	AAV Treated	13	AAV-Ink4a1-Ink4a2-Kras-Kras HA	2.2×10^{12}	1.29×10^{10}
					AAV-Tp53-Smad4-Brca2	1.5×10^{12}	1.29×10^{10}
			Control	5	Saline	-	-

3. Results

3.1 sgRNA cleavage activity test of SpCas9 and CjCas9 in C57BL/6 embryo

I targeted 5 genes, *Kras, Ink4a, Tp53, Smad4, Brca2* with two different cas9 orthologues including SpCas9 and CjCas9 for this study (Figure 10a). In SpCas9, *Kras, Tp53, Smad4 and Brca2* were targeted with single sgRNA and *Ink4a* were targeted with dual sgRNAs to induce premature termination codon(PTC) in 2 different alternative mRNA. Each of the delivery vector can cover 3 sgRNAs so *Kras, Ink4a1(exon1) and Ink4a2(exon2)* grouped as first vector and *Tp53, Smad4 and Brca2* grouped as second vector. Since SpCas9 size was 4.1kb which nearly fits to AAV packaging size, Cas9 vector was separately delivered.

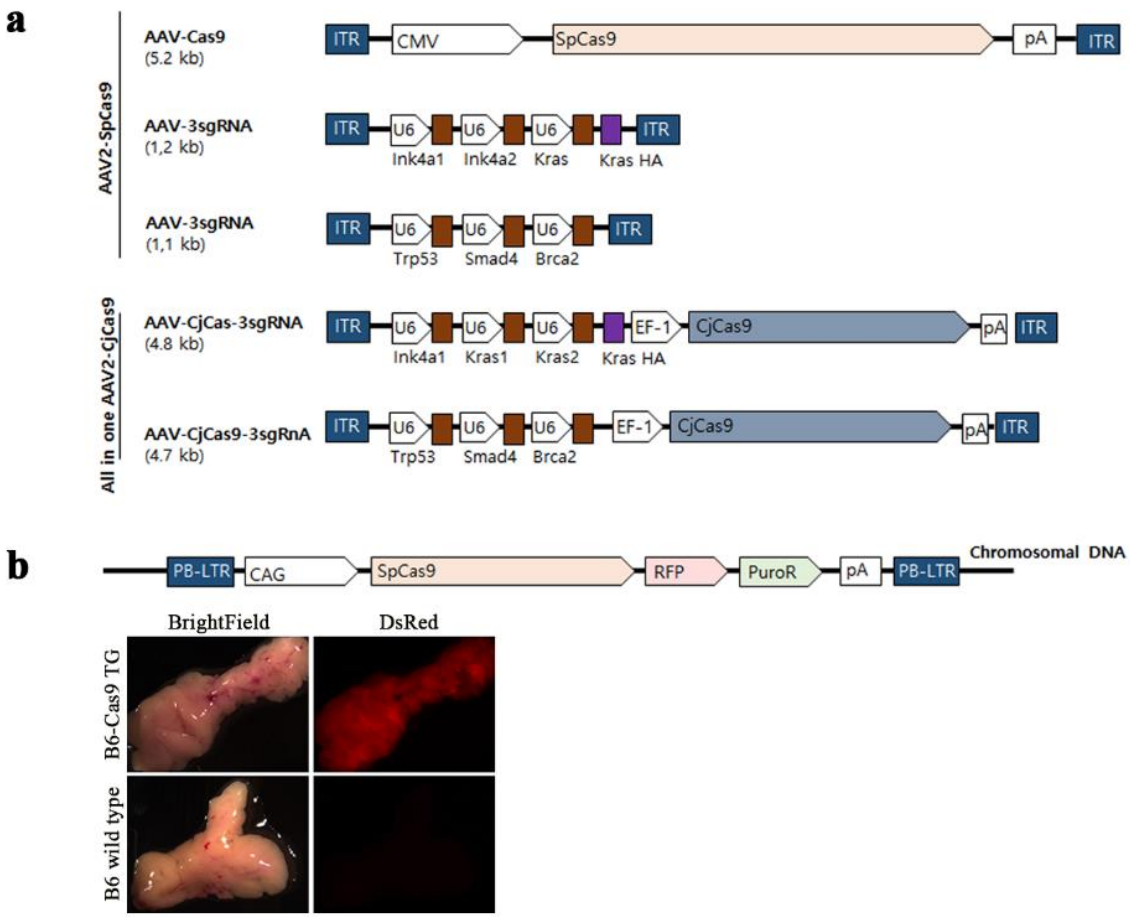
a
AAV2-SpCas9
AAV-Cas9
(5.2 kb)
ITR
CMV
SpCas9
pA
ITR
AAV-3sgRNA
(1,2 kb)
U6
Ink4a1
Ink4a2
Kras
Kras HA
AAV-3sgRNA
(1,1 kb)
Trp53
Smad4
Brca2
All in one AAV2-CjCas9
AAV-CjCas-3sgRNA
(4.8 kb)
EF-1
CjCas9
Kras1
Kras2
AAV-CjCas9-3sgRnA
(4.7 kb)
b
PB-LTR
CAG
RFP
PuroR
Chromosomal DNA
BrightField
DsRed
B6-Cas9 TG
B6 wild type

Figure 10. Schematic for pancreatic cancer modeling and Cas9 overexpression mouse. (a) Schematic of gene combinations for pancreas in vivo gene targeting. Three vectors, one containing SpCas9 and the others containing sgRNAs and gene of interest (GOI), were designed for SpCas9 mediated in vivo gene targeting and two vectors containing both GOI and CjCas9 were designed for CjCas9 mediated in vivo gene targeting. CMV: enhancer, pA: polyadenylation signal, U6: promoter, Kras HA: Kras Homology Arm, EF-1: EF-1-alpha core promoter **(b)** Cas9 overexpression mouse harboring genomic information. PB-pCAG-SpCas9/RFP-polyA was integrated into mouse allele by transposase. Cas9 expression was confirmed by RFP microscopy. Generated B6-Cas9 TG showed RFP signal and this elucidate Cas9 overexpression.

15ng/μl of each vector containg sgRNAs and 50ng/μl of SpCas9 vector was microinjected into mouse embryos. PCR and heteroduplex page assay on genomic DNA (gDNA) extracted from blastocysts of microinjected embryos revealed various cleavage efficiency by the gene which are *Kras (*87.5%, 7/8), *Ink4a1 (CdKn2a-ex1β) (*75%, 6/8), *Ink4a2 (CdKn2a-ex2) (*75%, 6/8), *Tp53 (*25%,2/8), *Smad4 (*37.5%, 3/8), *Brca2(*12.5%, 1/8) (Figure 11a).

By Using CjCas9, dual sgRNAs were used to increase knock-in efficiency and the other 4 genes were targeted with single sgRNA. Two sets of all-in-one vector containing both 3sgRNAs and CjCas9(2.9kb) were microinjected in 15ng/μl concentration into mouse embryos in plasmid form. PCR and heteroduplex page assay on genomic DNA (gDNA) extracted from blastocysts of microinjected embryos revealed in *Kras (*100%, 8/8), *Ink4a2 (CdKn2a-ex2) (*37.5%, 3/8), *Tp53(*50%, 4/8), *Smad4 (*37.5%, 3/8), *Brca2 (*12.5%, 1/8) gene respectively (Figure 11b). Although sgRNA sequences for SpCas9 and CjCas9 were different, targeting efficiency for each gene was similar.

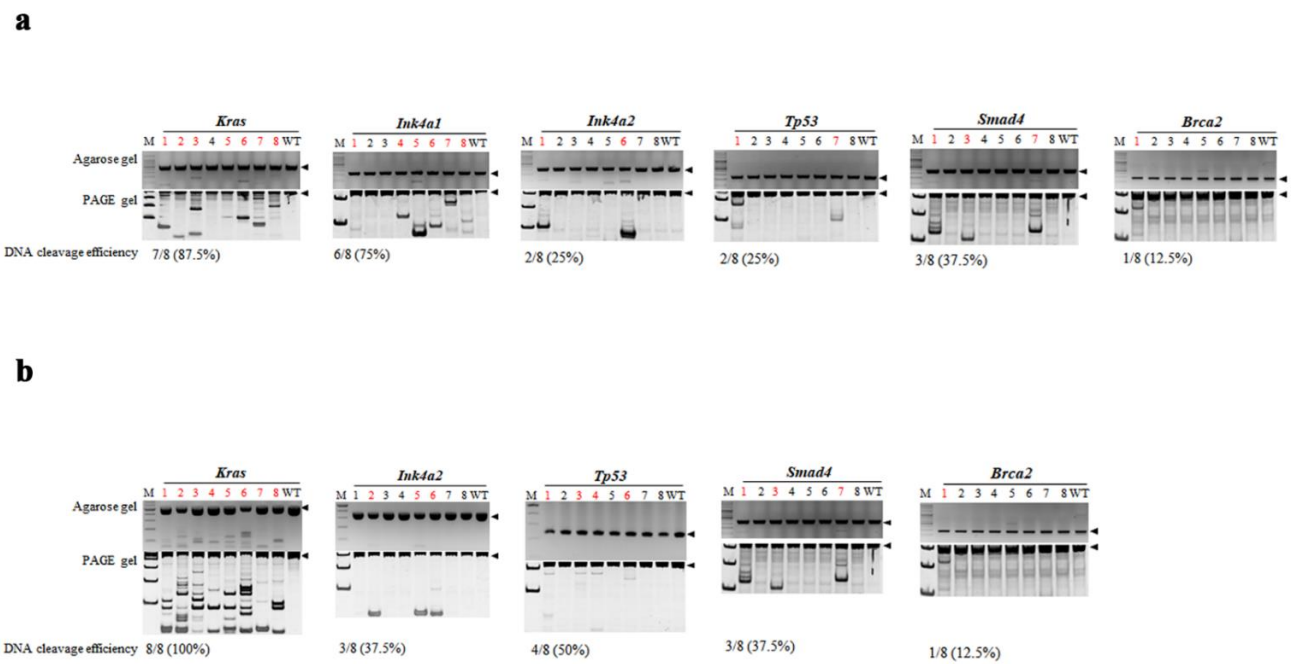

Figure 11 │ Evaluation of sgRNA efficacy. (a) psgRNA and Spcas9 mRNA were co-injected into 1-cell embryos and **(b)** pCjCas9-sgRNAs were injected into 1-cell embryos and DNA cleavage activity were evaluated by hetero-duplex formation and PAGE gel running. DNA cleavage efficiency were ranged from 12.5%-100%. Red letter indicates DNA cleaved blastocyst and black arrow indicates size of each PCR product and detail information were in Table 11.

Table 11. PCR Primer sets for genotyping.

Primer	Size	Forward sequence	Reverse sequence
Kras	530	ACGCAGACTGTAGAGCAG	AAGGGTAGGTGTTGGGATAG
Ink4a-1	259	GCCTTTCCTACCTGGTCCA	GCTTCTCACCTCGCTTGTC
Ink4a-2	365	TGGGTTGCTTCTTCTTTTTCTG	CTCTTCTGCTCAACTACGGT
Tp53	249	TTGGGCTTTGGTGTTGGG	AGGGACAAAAGATGACAGGG
Smad4-SpCas9	395	GGAGGAAGCAGGCCAAGAA	GGCTGGTCGGAAAGGATT
Brca2-SpCas9	286	ACTCAGGTTGTCAGGCAC	AAACTGATGGTAGGGGGGA
Smad4-CjCas9	792	TTGAGGTAAAGGCACATTTGG	TGCTCTCTTCTCGCCTCT
Brca2-CjCas9	484	TTTTGGCCACGTACCTTCT	CTCACAACCACCCGAAACT

3.2 SpCas9 expression was confirmed by RFP signal in pancreas

In previous report about delivery of AAV-SpCas9, they were packaged into single AAV vector[63, 64] or split into two parts[65, 66]. However, co-delivery is less efficient than the delivery of a single AAV vector *in vivo* and split spCas9 is less active than the intact SpCas9[67, 68]. To reduce such issues, I generated SpCas9 overexpression mouse by microinjection with transposase and PB-pCAG-SpCas9/RFP-polyA vector into C57BL/6 mouse embryos. After obtaining sufficient transgenic mouse, various organs were imaged by RFP wave length. Brain, eye muscle, pancreas, leg muscle expressed RFP signal which elucidate SpCas9 overexpression (Figure 10b and Figure 12). Whereas, Lung, liver, spleen, stomach, duodenum, intestine, kidney, lipid and testis (in male) didn't expressed RFP signal. Since pancreas expresses SpCas9 I decided to use this strain for AAV-3sgRNA injection.

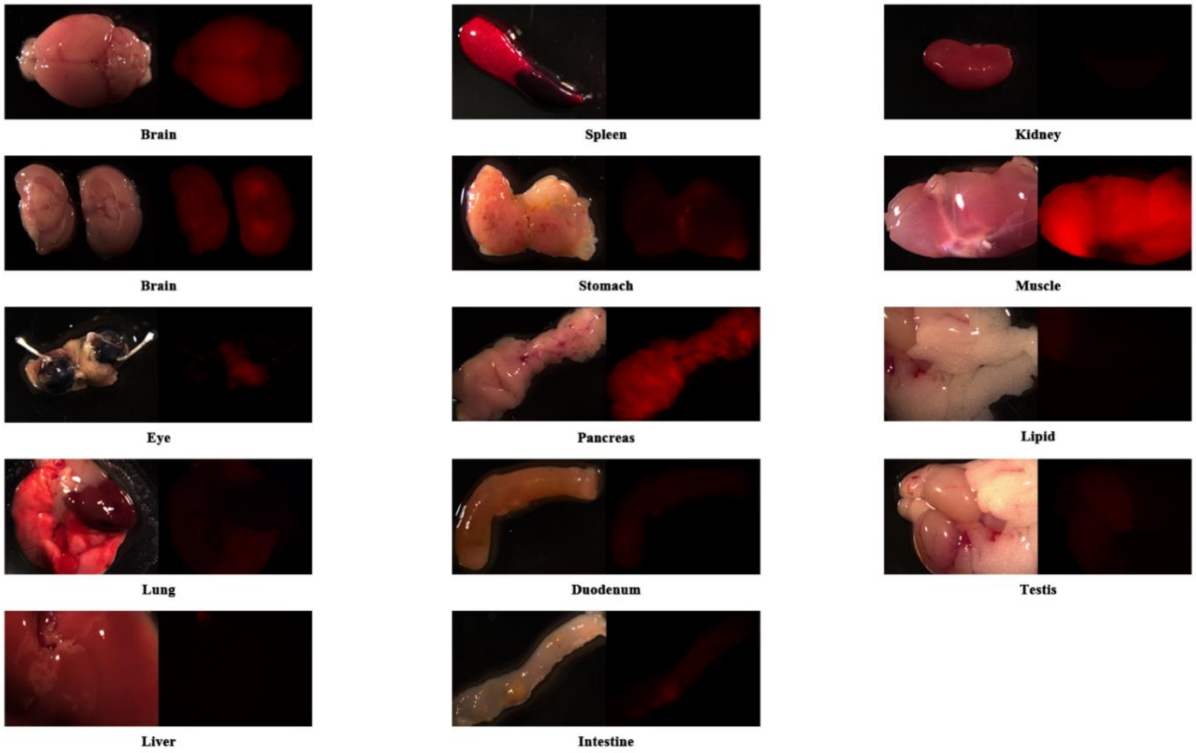

Figure 12. Cas9 overexpression mouse validation by RFP signal. PB-pCAG-SpCas9/RFP-polyA vector was used. So RFP signal elucidate overexpression of SpCas9. Brain, Pancreas, Muscle showed SpCas9 overexpression.

3.3 In vivo Pancreas-tropism of AAV2

One of the ultimate goals of successful *in vivo* gene targeting is to be able to deliver a gene of interest directly into the body. Compare to other AAV serotypes, AAV2 has been reported for diverse tissue-tropism[69]. However, by the species and strain tissue-tropisms are quite different so I examined AAV2 pancreas-tropism in C57BL/6 and FVB mouse strain by directly injecting GFP packaging adeno-associated virus (AAV-GFP) into common bile duct of pancreas. Injection solution contains 1.29×10^{10} viral particle with 0.5% trypan blue which diluted in saline up to 200μl. After 3-7week of surgery, liver to pancreas and duodenum was dissected and organ was observed by fluorescence microscope. GFP was detected in dispersed region of pancreas and surgery after 3-4week mice (C57BL/6 and FVB) showed better GFP signal than 7week mice(FVB) (Figure 13 and Figure 14).

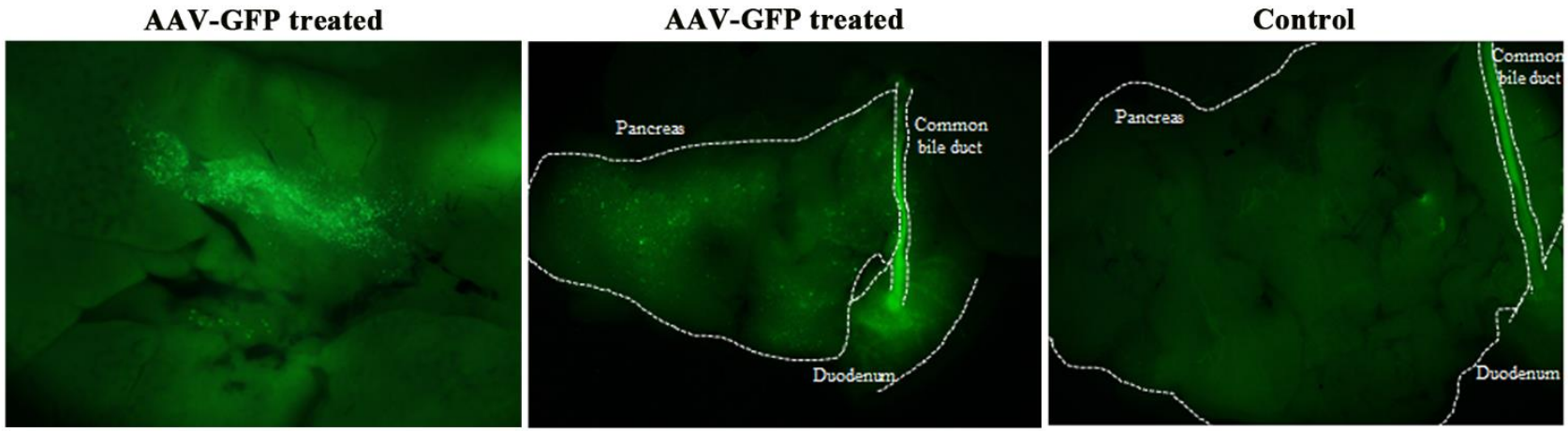

Figure 13. pAAV-GFP in vivo gene targeting ex vivo imaging. AAV-GFP were injected to C57BL/6 and FVB mouse. GFP imaging was conducted 4weeks post-surgery in C57BL/6 (Left panel) and 3weeks post-surgery in FVB (Right panel). AAV-GFP injected mice showed dispersed GFP expression over the pancreas (Left and mid panel). Control mouse showed none of the GFP expression in pancreas (Right panel). White guideline distinguishes each of the organs.

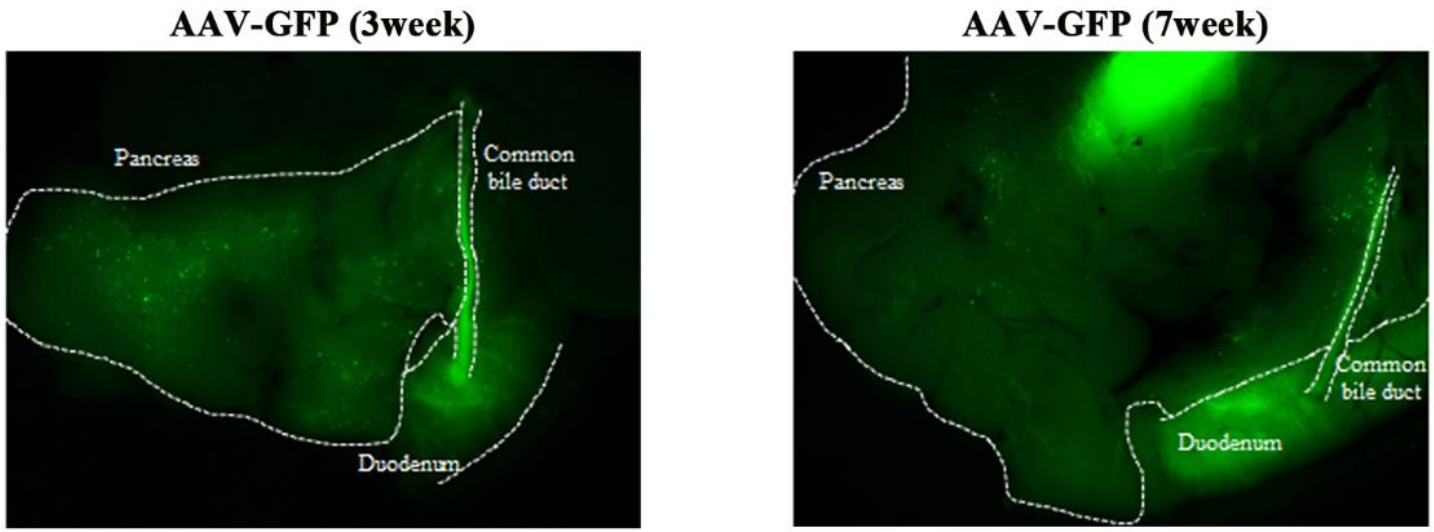

Figure 14. pAAV-GFP in vivo gene targeting ex vivo imaging. AAV-GFP were injected to FVB mouse. Left panel was imaged 3week post-surgery (Fig 13) and Right panel was imaged 7week post-surgery. Both expressed GFP but 3week post-surgery image showed more intense GFP signal.

3.4 Monitoring

Surgery has been successfully completed and monitoring is conducted every week. Until now any specific appearance of symptoms such as jaundice by gallbladder obstruction, drastic weight loss, hunching and shrinking are not found. For PDAC formation, accumulation of mutant cells that edited by AAV mediated CRISPR/Cas9 system have to be occur and that will take at least 10 months so studies are ongoing.

4. Discussion

Previously, due to multi-gene mutation have to be occur for pancreas adenocarcinoma it was nearly impossible to generate the appropriate model. However, our study suggests possibility to mutate multiplex genome in adult wild type mouse by directly injecting AAV into the pancreas. This will induce cancer, which will provide access to the genetic complexity of pancreatic cancer. Furthermore, various cancers are related with multi gene mutation and this technique will enlarge the complex cancer research.

In this study three scenarios were designed, including (i) tri-co-transduction with AAV2-Spcas9 and two sets of AAV2-3sgRNAs into wild type (WT) mouse, (ii) dual-co-transduction with two AAV2-3sgRNAs into SpCas9 overexpression mouse and (iii) dual-co-transduction of two AAV2-CjCas9-3sgRNAs into wild type(WT) mouse. Tri-co-transduction into WT mouse is a classical way of *in vivo* gene targeting but because three AAVs competitively transduce single cell and this can eventually decline DSB rate. Dual-co-transduction into Cas9 overexpression mouse is an alternative way which can reduce competitiveness with AAV2-SpCas9. Dual-co-transduction into WT mouse using all-in-one vector is a firstly used methods and I expected this would be the best way for efficient DSB induction. This has no need for competing AAV2-Cas9 with AAV2-sgRNAs and because I used WT mouse it saves endeavor for generating Cas9 overexpression mouse which can be further applicable for other *in vivo* gene targeting.

Before implementing three scenarios, DSB activities of SpCas9 and CjCas9 mediated sgRNAs were verified and the result overall ranged from 12.5% to 100%. In detail, comparing same gene that targeted with different orthologue cas9 showed similar cleavage rate. This demonstrates cleavage rate also dependent on genomic locus not only in sgRNA ability. For adenocarcinoma formation simultaneous multi gene mutation has to be followed so cleavage efficiency should be high. However, some of the gene I targeted such as Brca2 showed low DSB rate which was identical as previous[70-72] report. This can be overcome by virus characteristic which are consistently expresses its containing Cas9 along with sgRNA expression cassettes and necessary genetic elements (i.e., promoters and polyadenylation sequences) and eventually leads to DSB.

Most recently, Platt *et al*. generated Cre-dependent Cas9 overexpression mouse and suggested that these can facilitate causal genetic mutations in disease processes[73]. I also produced Cas9 overexpression mouse for efficient AAV transduction *in vivo*. Instead of Cre-dependent, transposon piggybac system was applied for inserting multiple copies of exogenous DNA fragment into mammalian genomes[74, 75]. SpCas9 overexpression was confirmed by imaging RFP which was tagged with SpCas9. In fact, I generated two mouse strain which were C57BL/6 and FVB but as the germline transmission was proceeded FVB showed decreased RFP signal whereas C57BL/6 showed steady signal of RFP. Albeit C57BL/6 has cancer resistance I used this strain for AAV transduction. Furthermore, in C57BL/6

pancreas as well as muscle showed intense signal and this could suggest the application for further muscle research.

AAV is currently the leading candidate for virus-based gene manipulation because of their broad tissue tropism, non-pathogenic nature and low immunogenicity[76]. One of the many serotypes, AAV2 which used in this study entry the cell by heparan sulfate proteoglycan(HSPG) as a primary receptor[77, 78] while FGFR1[79] and αvβ5 integrin[80] serve as co-receptors. Primary receptor HSPG, a kind of glycoprotein, is an important component of basement membrane which is relevant to all cells and because of this specific tissue gene editing would be difficult. To confirm both AAV2-tropism in pancreas and local transduction, AAV2-GFP was locally injected by closing cystic duct near gallbladder to prevent influx of the virus into the liver. This local injection showed clear expression only in pancreas and this method might express viral element in long-term than intra-vein injection which disperse to whole body.

The ultimate goal of this study is to observe successful pancreatic mouse modeling by *in vivo* genome editing. Though I have confirmed possibility of PDAC formation, cancer phenotype in mouse hasn't yet been detected. This is because not only mutation by AAVs containing editing molecule but also accumulation of mutant cells leads to carcinoma. I expect PDAC formation outsets at least 9 months after surgery so further histopathological research will be conducted. Also, comparing

delivery tools (lipofectamine, ribonucleoprotein electroporation) by targeting same locus haven't attempted. This could establish best system for *in vivo* gene targeting.

To recapitulate, multi gene related pancreatic cancer modeling using CRISPR/Cas9 system with AAV2 virus facilitate various cancer modeling that had not been established and also enables direct gene editing in wild type adult mouse which can applied to gene therapy. In this study, species are localized in mouse but this shows prospect of disease research in broader species such as in mid · large animals.

References

1. Gaj, T., C.A. Gersbach, and C.F. Barbas, 3rd, *ZFN, TALEN, and CRISPR/Cas-based methods for genome engineering.* Trends Biotechnol, 2013. **31**(7): p. 397-405.
2. Al-Attar, S., et al., *Clustered regularly interspaced short palindromic repeats (CRISPRs): the hallmark of an ingenious antiviral defense mechanism in prokaryotes.* Biol Chem, 2011. **392**(4): p. 277-89.
3. Deveau, H., J.E. Garneau, and S. Moineau, *CRISPR/Cas system and its role in phage-bacteria interactions.* Annu Rev Microbiol, 2010. **64**: p. 475-93.
4. Horvath, P. and R. Barrangou, *CRISPR/Cas, the immune system of bacteria and archaea.* Science, 2010. **327**(5962): p. 167-70.
5. Karginov, F.V. and G.J. Hannon, *The CRISPR system: small RNA-guided defense in bacteria and archaea.* Mol Cell, 2010. **37**(1): p. 7-19.
6. Makarova, K.S., et al., *Evolution and classification of the CRISPR-Cas systems.* Nat Rev Microbiol, 2011. **9**(6): p. 467-77.
7. Marraffini, L.A. and E.J. Sontheimer, *CRISPR interference: RNA-directed adaptive immunity in bacteria and archaea.* Nat Rev Genet, 2010. **11**(3): p. 181-90.
8. Andersson, A.F. and J.F. Banfield, *Virus population dynamics and acquired virus resistance in natural microbial communities.* Science, 2008. **320**(5879): p. 1047-50.
9. Barrangou, R., et al., *CRISPR provides acquired resistance against viruses in prokaryotes.* Science, 2007. **315**(5819): p. 1709-12.
10. Liu, T., et al., *Development and potential applications of CRISPR-Cas9 genome editing technology in sarcoma.* Cancer Lett, 2016. **373**(1): p. 109-118.
11. van der Oost, J., et al., *Unravelling the structural and mechanistic basis of CRISPR-Cas systems.* Nat Rev Microbiol, 2014. **12**(7): p. 479-92.
12. Cong, L., et al., *Multiplex genome engineering using CRISPR/Cas systems.* Science, 2013. **339**(6121): p. 819-23.
13. Ozeki, H., et al., *Spectrophotometric characterization of eumelanin and*

pheomelanin in hair. Pigment Cell Res, 1996. **9**(5): p. 265-70.

14. Tran, M.T., et al., *In vivo image analysis using iRFP transgenic mice.* Exp Anim, 2014. **63**(3): p. 311-9.
15. Labun, K., et al., *CHOPCHOP v2: a web tool for the next generation of CRISPR genome engineering.* Nucleic Acids Res, 2016. **44**(W1): p. W272-6.
16. Liu, Y., et al., *Molecular basis for hair loss in mice carrying a novel nonsense mutation (Hrrh-R) in the hairless gene (Hr).* Vet Pathol, 2010. **47**(1): p. 167-76.
17. Panteleyev, A.A., R. Paus, and A.M. Christiano, *Patterns of hairless (hr) gene expression in mouse hair follicle morphogenesis and cycling.* Am J Pathol, 2000. **157**(4): p. 1071-9.
18. Strozik, E. and M.F. Festing, *Whisker trimming in mice.* Lab Anim, 1981. **15**(4): p. 309-12.
19. Balciunaite, G., et al., *Wnt glycoproteins regulate the expression of FoxN1, the gene defective in nude mice.* Nat Immunol, 2002. **3**(11): p. 1102-8.
20. Schorpp, M., et al., *Characterization of mouse and human nude genes.* Immunogenetics, 1997. **46**(6): p. 509-15.
21. Flanagan, S.P., *'Nude', a new hairless gene with pleiotropic effects in the mouse.* Genet Res, 1966. **8**(3): p. 295-309.
22. Potter, G.B., et al., *The hairless gene mutated in congenital hair loss disorders encodes a novel nuclear receptor corepressor.* Genes Dev, 2001. **15**(20): p. 2687-701.
23. Miller, J., et al., *Atrichia caused by mutations in the vitamin D receptor gene is a phenocopy of generalized atrichia caused by mutations in the hairless gene.* J Invest Dermatol, 2001. **117**(3): p. 612-7.
24. Reske-Kunz, A.B., M.P. Scheid, and E.A. Boyse, *Disproportion in T-cell subpopulations in immunodeficient mutant hr/hr mice.* J Exp Med, 1979. **149**(1): p. 228-33.
25. Morrissey, P.J., et al., *Immunologic abnormalities in HRS/J mice. I. Specific deficit in T lymphocyte helper function in a mutant mouse.* J Immunol, 1980. **125**(4): p. 1558-62.
26. Suzu, S., et al., *p56(dok-2) as a cytokine-inducible inhibitor of cell proliferation and signal transduction.* EMBO J, 2000. **19**(19): p. 5114-22.
27. Thompson, S., et al., *Germ line transmission and expression of a corrected*

HPRT gene produced by gene targeting in embryonic stem cells. Cell, 1989. **56**(2): p. 313-21.

28. Wiedenheft, B., S.H. Sternberg, and J.A. Doudna, *RNA-guided genetic silencing systems in bacteria and archaea.* Nature, 2012. **482**(7385): p. 331-8.
29. Jinek, M., et al., *A programmable dual-RNA-guided DNA endonuclease in adaptive bacterial immunity.* Science, 2012. **337**(6096): p. 816-21.
30. Hsu, P.D., E.S. Lander, and F. Zhang, *Development and applications of CRISPR-Cas9 for genome engineering.* Cell, 2014. **157**(6): p. 1262-78.
31. Sander, J.D. and J.K. Joung, *CRISPR-Cas systems for editing, regulating and targeting genomes.* Nat Biotechnol, 2014. **32**(4): p. 347-55.
32. Zhang, X., et al., *Efficient Production of Gene-Modified Mice using Staphylococcus aureus Cas9.* Sci Rep, 2016. **6**: p. 32565.
33. Kim, Y., et al., *Generation of knockout mice by Cpf1-mediated gene targeting.* Nat Biotechnol, 2016.
34. Hur, J.K., et al., *Targeted mutagenesis in mice by electroporation of Cpf1 ribonucleoproteins.* Nat Biotechnol, 2016.
35. Ran, F.A., et al., *In vivo genome editing using Staphylococcus aureus Cas9.* Nature, 2015. **520**(7546): p. 186-91.
36. Zetsche, B., et al., *Cpf1 is a single RNA-guided endonuclease of a class 2 CRISPR-Cas system.* Cell, 2015. **163**(3): p. 759-71.
37. Fonfara, I., et al., *Phylogeny of Cas9 determines functional exchangeability of dual-RNA and Cas9 among orthologous type II CRISPR-Cas systems.* Nucleic Acids Res, 2014. **42**(4): p. 2577-90.
38. Hooton, S.P. and I.F. Connerton, *Campylobacter jejuni acquire new host-derived CRISPR spacers when in association with bacteriophages harboring a CRISPR-like Cas4 protein.* Front Microbiol, 2014. **5**: p. 744.
39. Kim, E., et al., *In vivo genome editing with a small Cas9 orthologue derived from Campylobacter jejuni.* Nat Commun, 2017. **8**: p. 14500.
40. Yamada, M., et al., *Crystal Structure of the Minimal Cas9 from Campylobacter jejuni Reveals the Molecular Diversity in the CRISPR-Cas9 Systems.* Mol Cell, 2017. **65**(6): p. 1109-1121 e3.
41. Ma, E., et al., *Single-Stranded DNA Cleavage by Divergent CRISPR-Cas9 Enzymes.* Mol Cell, 2015. **60**(3): p. 398-407.

42. Schaefer, K.A., et al., *Unexpected mutations after CRISPR-Cas9 editing in vivo.* Nat Methods, 2017. **14**(6): p. 547-548.
43. Ma, H., et al., *Correction of a pathogenic gene mutation in human embryos.* Nature, 2017. **548**(7668): p. 413-419.
44. Petris, M.J., D. Strausak, and J.F. Mercer, *The Menkes copper transporter is required for the activation of tyrosinase.* Hum Mol Genet, 2000. **9**(19): p. 2845-51.
45. Tomita, Y., et al., *Human oculocutaneous albinism caused by single base insertion in the tyrosinase gene.* Biochem Biophys Res Commun, 1989. **164**(3): p. 990-6.
46. Stokowski, R.P., et al., *A genomewide association study of skin pigmentation in a South Asian population.* Am J Hum Genet, 2007. **81**(6): p. 1119-32.
47. Ryan , D.P., T.S. Hong , and N. Bardeesy *Pancreatic Adenocarcinoma.* New England Journal of Medicine, 2014. **371**(11): p. 1039-1049.
48. Bardeesy, N. and R.A. DePinho, *Pancreatic cancer biology and genetics.* Nat Rev Cancer, 2002. **2**(12): p. 897-909.
49. Waddell, N., et al., *Whole genomes redefine the mutational landscape of pancreatic cancer.* Nature, 2015. **518**(7540): p. 495-501.
50. Hruban, R.H., et al., *Pancreatic intraepithelial neoplasia: a new nomenclature and classification system for pancreatic duct lesions.* Am J Surg Pathol, 2001. **25**(5): p. 579-86.
51. Van Dyke, T. and T. Jacks, *Cancer modeling in the modern era: progress and challenges.* Cell, 2002. **108**(2): p. 135-44.
52. Lynch, H.T., et al., *Familial pancreatic cancer: clinicopathologic study of 18 nuclear families.* Am J Gastroenterol, 1990. **85**(1): p. 54-60.
53. Hruban, R.H., et al., *Genetics of pancreatic cancer. From genes to families.* Surg Oncol Clin N Am, 1998. **7**(1): p. 1-23.
54. Del Chiaro, M., et al., *Cancer risk among the relatives of patients with pancreatic ductal adenocarcinoma.* Pancreatology, 2007. **7**(5-6): p. 459-69.
55. Hruban, R.H., et al., *Update on familial pancreatic cancer.* Adv Surg, 2010. **44**: p. 293-311.
56. Chiou, S.H., et al., *Pancreatic cancer modeling using retrograde viral vector delivery and in vivo CRISPR/Cas9-mediated somatic genome*

editing. Genes Dev, 2015. **29**(14): p. 1576-85.

57. Sanchez-Rivera, F.J., et al., *Rapid modelling of cooperating genetic events in cancer through somatic genome editing.* Nature, 2014. **516**(7531): p. 428-31.
58. Platt, R.J., et al., *CRISPR-Cas9 knockin mice for genome editing and cancer modeling.* Cell, 2014. **159**(2): p. 440-55.
59. Xue, W., et al., *CRISPR-mediated direct mutation of cancer genes in the mouse liver.* Nature, 2014. **514**(7522): p. 380-4.
60. Zuckermann, M., et al., *Somatic CRISPR/Cas9-mediated tumour suppressor disruption enables versatile brain tumour modelling.* Nat Commun, 2015. **6**: p. 7391.
61. Maresch, R., et al., *Multiplexed pancreatic genome engineering and cancer induction by transfection-based CRISPR/Cas9 delivery in mice.* Nat Commun, 2016. **7**: p. 10770.
62. Ran, F.A., et al., *Genome engineering using the CRISPR-Cas9 system.* Nat Protoc, 2013. **8**(11): p. 2281-2308.
63. Long, C., et al., *Postnatal genome editing partially restores dystrophin expression in a mouse model of muscular dystrophy.* Science, 2016. **351**(6271): p. 400-3.
64. Swiech, L., et al., *In vivo interrogation of gene function in the mammalian brain using CRISPR-Cas9.* Nat Biotechnol, 2015. **33**(1): p. 102-6.
65. Chew, W.L., et al., *A multifunctional AAV-CRISPR-Cas9 and its host response.* Nat Methods, 2016. **13**(10): p. 868-74.
66. Truong, D.J., et al., *Development of an intein-mediated split-Cas9 system for gene therapy.* Nucleic Acids Res, 2015. **43**(13): p. 6450-8.
67. Wright, A.V., et al., *Rational design of a split-Cas9 enzyme complex.* Proc Natl Acad Sci U S A, 2015. **112**(10): p. 2984-9.
68. Zetsche, B., S.E. Volz, and F. Zhang, *A split-Cas9 architecture for inducible genome editing and transcription modulation.* Nat Biotechnol, 2015. **33**(2): p. 139-42.
69. Srivastava, A., *In vivo tissue-tropism of adeno-associated viral vectors.* Curr Opin Virol, 2016. **21**: p. 75-80.
70. Sharan, S.K., et al., *Embryonic lethality and radiation hypersensitivity mediated by Rad51 in mice lacking Brca2.* Nature, 1997. **386**(6627): p.

804-10.

71. Suzuki, A., et al., *Brca2 is required for embryonic cellular proliferation in the mouse.* Genes & Development, 1997. **11**(10): p. 1242-1252.

72. Ludwig, T., et al., *Targeted mutations of breast cancer susceptibility gene homologs in mice: lethal phenotypes of Brca1, Brca2, Brca1/Brca2, Brca1/p53, and Brca2/p53 nullizygous embryos.* Genes & Development, 1997. **11**(10): p. 1226-1241.

73. Platt, R.J., et al., *CRISPR-Cas9 Knockin Mice for Genome Editing and Cancer Modeling.* Cell, 2014. **159**(2): p. 440-455.

74. Wilson, M.H., C.J. Coates, and A.L. George, Jr., *PiggyBac transposon-mediated gene transfer in human cells.* Mol Ther, 2007. **15**(1): p. 139-45.

75. Ding, S., et al., *Efficient transposition of the piggyBac (PB) transposon in mammalian cells and mice.* Cell, 2005. **122**(3): p. 473-83.

76. Kotterman, M.A. and D.V. Schaffer, *Engineering adeno-associated viruses for clinical gene therapy.* Nat Rev Genet, 2014. **15**(7): p. 445-51.

77. Summerford, C. and R.J. Samulski, *Membrane-associated heparan sulfate proteoglycan is a receptor for adeno-associated virus type 2 virions.* J Virol, 1998. **72**(2): p. 1438-45.

78. Pillay, S., et al., *An essential receptor for adeno-associated virus infection.* Nature, 2016. **530**(7588): p. 108-12.

79. Qing, K., et al., *Human fibroblast growth factor receptor 1 is a co-receptor for infection by adeno-associated virus 2.* Nat Med, 1999. **5**(1): p. 71-7.

80. Summerford, C., J.S. Bartlett, and R.J. Samulski, *AlphaVbeta5 integrin: a co-receptor for adeno-associated virus type 2 infection.* Nat Med, 1999. **5**(1): p. 78-82.

국문초록

생물학 분야에 엄청난 발전을 가져온 CRISPR/Cas 시스템은 유전자 편집에 강력한 도구로 사용되어왔다. CRISPR/Cas 타입 Ⅱ 중에서도, Streptococcus pyogene Cas9(SpCas9) 는 처음이자 가장 널리 사용되고 있는데 이는 DNA이중가닥을 자르는 효율이 높고 off-target 또한 낮기 때문이다. 최근에는 새로운 종인 Campylobacter jejuni Cas9 (CjCas9)에서 가장 작은 사이즈의 cas9을 가지고 있는 발표되었다. 이렇게 새로운 orthologue를 찾는 이유는 이것이 단지 새로운 타입의 CRISPR를 찾는데 에서 그치는 것이 아니라 질환동물모델링이나 유전자 치료 같은 다양한 분야의 적용에 대한 전망을 주기 때문이다. 결론적으로 이러한 모든 적용들의 궁극적인 목표는 사람에서 유전자 질병을 치료하기 위한 것이다. 따라서, 연구들이 발전함에 따라 CRISPR system의 높은 절단 효율뿐만 아니라 낮은 off-target이 강조되고 있다. 그래서 본연구에서는 널리 사용되고있는 SpCas9과 새로운 ortholgue인 CjCas9을 이용한 동물모델링을 통하여 효율, off-target에 대한 전반적인 연구를 진행하였다.

첫번째로는, SpCas9을 사용해서 hairless 마우스를 제작하였다. 간단하게 말하자면, 절단 효율이 배반포 단계에서 30%(3/10), 제작된 마우스에서 20-28.5%(1/5-2/7) 보였다. 제작된 돌연변이 마우스들 중 표현형 관찰을 위해 #1-4 (*Hr* 유전자 위치에 -3 과 -34 아미노산 결실)와 #2-4 (Hr 유전자 위치에 premature termination codon(PTC)와 -50 아미노산 결실) 마우스를 germline transmission을 내렸다. #1-4 마우스 라인의 경우에는 털이 빠지는 표현형이 나타나지 않았지만 #2-4 마우스 라인의 경우 생후 2주째부터 털이 빠지는 것을 관찰할 수 있었다. 본 연구에서는 SpCas9의 절단 효율을 입증했고 추가적으로 Hr 마우스의 경우 피부의학연구와 in vivo imaging에 적절한 모델이 될 수 있음을 제안한다.

Hr의 연구가 진행되던 중 앞에서 언급한 새로운 orthologue CjCas9에 대해 in vitro

연구까지 발표가 되었다. 비록 CjCas9의 절단 효율에 대해서 많은 의견이 존재했지만, CjCas9을 활용하여 절단 효율과 off-target 가능성을 in vivo 단계에서 조사하였다. 통틀어서, 배반포와 제작된 마우스에서 적게는 38% 많게는 100%의 절단 효율을 보였고 이는 예상 치에 비해 훨씬 높았다. 게다가, off-target 분석은 ≤1.6%로 높은 특이성을 보였다. 추가적으로 최근 Schaefer et al. 에서 바이오인포매틱스를 이용한 off-target 분석을 진행하였는데 그 결과 SpCas9이 높은 off-target을 지닌다고 보고하였다. 하지만 CjCas9을 사용한 본 연구 중에서 이는 Schaefer et al의 SpCas9으로 만든 돌연변이 마우스 시퀀스를 잘못된 컨트롤 마우스 시퀀스에 정렬했기 때문에 잘못되 해석을 했다고 밝혀냈다. 결론적으로, CjCas9은 높은 절단 효율과 높은 특이성을 보였고 이는 안전한 유전자 타겟팅을 가능케 할 수 있다고 제안한다.

효율적이고 정확성이 높은 CjCas9의 발견을 토대로, 추가적으로 여러 유전자가 연관되어 있는 췌장암 모델링을 아데노의존성 바이러스(AAV)를 통해 생체 내 유전자 적중을 진행하였다. 본 연구에서는 같은 유전자를 SpCas9과 CjCas9으로 타겟팅 함으로써 서로 간의 직접적인 비교를 하였다. 절단 효율은 수정란에서 검증이 되었고 SpCas9-mediated 와 CjCas9-mediated에서 비슷한 효율을 보였다. 그런 뒤, 생체 내 유전자 적중은 AAV에 쌓여진 molecule을 성체 마우스의 췌장 common bile duct에 직접적으로 주입됨으로써 진행되었다. 암 형성을 수술 후 최소 9개월이 소요되기 때문에 본 연구는 진행중에 있다.

결론적으로, 본 연구에서는 CjCas9의 안전하고 안정적인 능력을 다양한 방법을 통하여 동물 모델을 만듦으로써 입증하였다. 이는 CjCas9의 광범위한 활용성을 제시한다.